Application of high-power lasers to study matter at ultrahigh pressures

S. I. Anisimov, A. M. Prokhorov, and V. E. Fortov

L. D. Landau Institute of Theoretical Physics of the Academy of Sciences of the USSR, Chernogolovka (Moscow Province)

Institute of General Physics of the Academy of Sciences of the USSR

Institute of Chemical Physics of the Academy of Sciences of the USSR

Usp. Fiz. Nauk **142**, 395–434 (March 1984)

This article reviews the current status of studies by means of lasers of superdense nonideal plasmas. The main attention is paid to laser methods of generating plane steady-state shock waves with extremely high pressures. The role is discussed of various factors that complicate the design of laser experiments: generation of high-energy non-Maxwell electrons, plasma and hydrodynamic instabilities, restrictions on heat flux, etc. The advantages are pointed out of using high-frequency lasers and layered targets to obtain a plasma with extremal parameters.

TABLE OF CONTENTS

1. Introduction 181
2. Theoretical models and experimental studies of the thermodynamics of materials at high pressures and temperatures 182
3. Potentialities of lasers for generating high-power shock waves in condensed media 185
   a) Very simple estimates of the pressure in a plasma. b) Absorption of laser radiation. c) Energy transport by electronic heat conduction. d) Hydrodynamic instability of plasma compression. e) Numerical calculations and scaling relationships for the pressure of a shock-compressed plasma.
4. Structure of laser shock waves and general requirements on the design of targets.. 190
   a) Damping effects in the lateral and rear unloading waves. b) The effect of two-dimensional dispersal of the plasma corona. c) Formation of a quasistationary shock wave. d) Heating of the target by nonthermal electrons. e) Scaling relationships for homogeneous targets. f) Radial expansion of the energy-release region at high intensities. g) The "internal" structure of laser shock waves. h) Results of numerical simulation.
5. Diagnostics and experiments 198
   a) General requirements on targets and diagnostic means. b) Experiments with laser shock waves. c) Experiments on heating with fast electrons. Anomalous energy transport. d) Experiments on ablative acceleration.
6. Conclusions 203
References 203

1. INTRODUCTION

The high-power pulsed lasers constructed for purposes of controlled thermonuclear fusion offer a unique potentiality of generating light pulses with energy of 10^4 J and a power of tens of terawatts.[40,113] One can focus such pulses with optical systems into a spatial region of dimensions smaller than 100 μm, so that the resulting energy flux density reaches 10^{17} W/cm^2. When these pulses act on condensed media, record-setting local energy densities are obtained that currently can not be obtained under laboratory experimental conditions by any other methods. This situation makes high-power laser systems a very promising instrument for studying matter in the plasma state at extremely high pressures and temperatures. Hydrodynamic calculations partially confirmed now by experiments to measure the parameters of the dispersing plasma, its x-ray emission and neutron yield, imply that in the traditional "thermonuclear" design of the experiment pressures of hundreds of megabars should be attained in the inner regions of spherical laser targets. These are comparable in order of magnitude with the atomic pressure unit $e^2/a_B^4 = 300$ Mbar $= 3\times 10^8$ atm. The laser intensities needed to obtain such pressures lie in the working range of already existing laboratory apparatus. However, in this case the measurement of the parameters of the compressed matter is an extremely complex problem. This is partly due to the small spatial dimensions, the strong inhomogeneity, and the short time of existence of the matter in the strongly compressed state. In principle, this difficulty can be overcome by increasing the energy of the laser. However, we can easily see that the needed energy is proportional to the cube of the characteristic dimension (or, equivalently, the cube of the inertial confinement time). Therefore the practical possibilities of increasing the scale of the experiments are highly restricted. Another difficulty in the diagnostics of compresses and heated matter arises from the very geometry of the spherical laser experiments, in which the compressed inner layers of the target are "screened" by the hot and relatively rarefied diverging plasma of the corona.

 0038-5670/84/030181-25$01.80

The diagnostics is substantially simplified in going to a planar geometry of compression, since then one can use the laws of conservation of mass, momentum, and energy to determine the parameters of the compressed matter. In the case of a one-dimensional quasistationary flow, these have the very simple form of a system of algebraic equations. An approach based on applying the conservation laws to a stationary shock explosion is fundamental in the dynamic physics of high pressure. It has been successfully applied to study the thermodynamic and kinetic properties of materials in the megabar pressure range. Here chemical explosives or light-gas propellant apparatus was used to generate the shock waves. A fundamental contribution to the development of this field of studies was introduced by the pioneer studies of Ya. B. Zel'dovich, L. V. Al'tshuler, S. B. Kormer, and other scientists. The fundamentals of the method and the most important results are presented in the review of articles of Refs. 1–4 and the monograph of Ref. 5.

The application of high-power lasers to generate shock waves allows one to extend substantially the range of attainable pressures. Understandably, in laser experiments the classical approach based on using plane, quasistationary shock waves is also the most promising for performing quantitative measurements. Up to now a large part of the experiments on laser generation of high-power shock waves has been performed precisely in this traditional design, which imposes definite restrictions on the parameters of the target and the laser pulse. In this design, one can now generate in metals plane laser shock waves with a pressure behind the front of tens of megabars, which exceeds by severalfold the values attainable in the traditional technique of condensed explosives and light-gas "guns," and is comparable only with the pressures that are attained in the near zone of underground nuclear explosions.

This article reviews the studies on obtaining extremely high pressures with lasers and an attempt is made to evaluate the potentialities of using lasers to study the dynamic physics of high pressures. We shall be interested primarily in determining the equation of state and other thermodynamic characteristics of a superdense plasma, although the laser experiments make it possible in principle to obtain also more extensive physical information. Section 2 carries out a brief analysis of the theoretical models and experimental data on the thermodynamics of materials in the megabar range of pressures that enables one to choose models most suitable for hydrodynamic calculations of flows with shock waves caused by high-power laser pulses. Subsequent comparison with experiment enables one to decide on the applicability of models and to determine their parameters. Section 3 estimates the maximum pressures that one can hope to obtain in experiments with the existing and projected laser systems based on CO_2 and neodymium glass, and also discusses the problem of using the short-wavelength harmonics of neodymium-laser radiation. The spatial and time structure of flows with shock waves generated by laser radiation is discussed in Sec. 4, which studies the effects of damping from the lateral and rear unloading waves, radiative and electronic energy transport in the wave front, and effects of inhomogeneity and other methodological problems. Special attention is paid to the influence of nonthermal electrons that arise in the absorption zone and the heating by these electrons of the target ahead of the wave, as well as a possible infuence of anomalous transport processes in the corona. On the basis of these data, Sec. 5 estimates the dimensions of laser targets and analyzes the advantages of layered systems, and also of the use of short-wavelength laser radiaiton. Section 6 evaluates the possible schemes of dynamic diagnostics and formulates the requirements on high-speed recording systems. The experiments performed up to now on laser generation of shock waves are discussed, together with possible laser experiments on isentropic compression and expansion of a plasma, detection of nonthermal electrons, and generation of harmonics of laser radiation.

2. THEORETICAL MODELS AND EXPERIMENTAL STUDIES OF THE THERMODYNAMICS OF MATERIALS AT HIGH PRESSURES AND TEMPERATURES

The recent decades are characterized by rapid progress in high-pressure physics[1–4,78,79] arising both from problems of promising technology (synthesis of the diamond phases of graphite and boron nitride, explosive, electron-beam, and laser welding and treatment of metals, etc.) and from the need for designing pulsed energy systems operating at record-setting high energy concentrations.[26] Moreover, studies in the field of megabar pressures substantially expand our physical concepts of the fundamental properties of matter in a broad and little-studied region of the phase diagram. In analyzing the physical conditions and hydrodynamic consequences of high-power pulsed energy release in condensed matter, greatest interest is offered by the equation of state—the fundamental characteristic of matter that determines the possibility of application of the formal apparatus of gasdynamics and thermodynamics to concrete physical systems.[4]

The fundamental difficulty of systematic theoretical determination of the equation of state of condensed matter by the methods of statistical physics involves the need for correctly taking into account the strong and structurally complicated interparticle interaction. No general methods for solution of this problem currently exist. Therefore one must introduce schematization in concrete calculations and study simplified models whose region of applicability proves restricted and is established in each concrete case by comparing either with more exact calculations or with the results of experiment. Another approach to the problem of equations of state consists in drawing on experimental data for choosing the numerical parameters in functional relationships constructed on the basis of the rigorous asymptotic solutions. The laser experiments discussed in this article are directed toward solving both these problems. They make it possible in principle to establish the limits of applicability of the asymptotic theories, and also to construct semiempirical models of the equation of state in the ultramegabar pressure region.

In the phase diagram of a material (see Figs. 1 and 2 in Ref. 3), the ideal gas occupies the region of relatively low temperatures and low densities, where the interparticle in-

teraction is weak and is taken into account within the framework of the virial equation of state. One can describe a substantially larger range of densities by the approximate methods developed in the theory of liquids; the method of integral equations, the pseudopotential method, the methods of molecular dynamics and the Monte Carlo method using computer simulation.[6] However, the reliable experimental data needed for a warranted choice of the pseudopotential and for checking the accuracy of the approximate methods at high pressures and temperatures are lacking. This hinders to a considerale extent the development of realistic models of a liquid that are valid up to the critical region or to the transition of the liquid to a plasma phase. Reducing the temperature of the liquid causes it to freeze and form a crystalline state. The properties of the latter are determined by the concrete shell structure and character of the filling of the electron energy bands, and also by the crystal-lattice symmetry. Classification of the possible state here is very complex, while a description of the varied situations requires the modern methods of solid-state theory, which has been well developed for calculating states at normal temperatures, but which lacks verification at high pressures and temperatures. However, we should note that the equations of state of crystalline objects are usually not very sensitive to the concrete structure of the crystal lattice,[4] and this sensitivity usually becomes smaller with higher pressure. For many dielectric crystals at a pressure of the order of 1–10 Mbar, the electrons become collectivized with transition to the metallic state, in which the free electrons make a considerable contribution to the total pressure.

The most extensive region of states in the phase diagram belongs to the plasma—the most widespread state of matter in nature. A solid, liquid, or gaseous material transforms to the plasma state as the result of thermal ionization (at $T > 10Z^{4/3}$ eV) or ionization by pressure (at a density $n_i > 1.6\times 10^{24} Z^3 N^{-6}$ cm^{-3}, where Z is the nuclear charge and N is the principal quantum number). The physical properties of an electron plasma are characterized by the nonideality parameter $\Gamma = e^2/\rho_D \mathscr{E}_k$ (ρ_D is the screening radius $= \sqrt{\mathscr{E}_k/4\pi n e^2}$, $\mathscr{E}_k$ is the kinetic energy) that describes the Coulomb interaction, and by the degeneracy parameter $n\lambda_e^3$ ($\lambda_e = \hbar/\sqrt{2\pi m T}$), which determines the quantum effects. In the high-temperature region the quantum effects are not very substantial, $n\lambda_e^3 \ll 1$, while the kinetic energy $\mathscr{E}_k \sim T$ exceeds the characteristic Coulomb energy e^2/ρ_D and we have $\Gamma \ll 1$. This enables one to use the model of an ideal Boltzmann plasma, which describes the ionization equilibrium within the framework of a "chemical" model (Saha). Upon isothermal compression of the Boltzmann plasma, the effects of Coulomb interaction in it are enhanced ($\Gamma \gtrsim 1$). This greatly hinders the theoretical description of the nonideal plasma. An important point is that electrons exist in free and bound states in such a plasma. This leads to additional complications involving the existence of a discrete spectrum of the strongly compressed medium. One must introduce complicated quantum-mechanical calculations to determine it, usually carried out by various approximate methods, in particular, the self-consistent field method.

The models proposed for this field[4] are based on extrapolations of the asymptotic theories. For this purpose they employ the as yet extremely few experiments on nonideal plasmas.[3] Compression of a plasma to densities corresponding to degeneracy leads to increased nonideality. Further, at densities $n_e > \lambda_e^{-3}$ the degeneracy of the electronic component leads to a more rapid growth in the kinetic energy than in the interaction energy, and to a diminished relative role of the interparticle interaction (the kinetic energy is $\mathscr{E}_k \sim \mathscr{E}_F \sim \hbar^2 m^{-1} n^{2/3}$, and the Coulomb energy is $\mathscr{E}_c \sim e^2 n^{1/3}$). In this region of ultrahigh pressures $p > 5\times 10^2 Z^{10/3}$ Mbar, the increase in density "simplifies" the properties of the degenerate plasma. The thermodynamics of such a plasma is described well by the model of an ideal Fermi gas, which has been exhaustively studied by analytic and numerical methods. At lower compressions of the material one must take into account effects of inhomogeneity caused by the electron-ion interaction, which leads to the Thomas-Fermi model, which amounts to a quasiclassical approximation to the method of the self-consistent field.[7] In this approximation, which is based on a cellular model, one assumes that the electron shells of the atoms become "crushed" under the extremely high pressures and a quasiuniform electron-density distribution is realized within the Wigner-Seitz unit cell. Owing to the relative simplicity of its calculations procedure and the self-preserving nature of the results in terms of the nuclear charge Z, this model, when supplemented by quantum and exchange corrections,[7] has become considerably widespread in high-pressure physics. In terms of the approximations made, the Thomas-Fermi model is applicable at pressures $p \gg 300$ Mbar and $T \gg \mathrm{Ry} \approx 14$ eV. At the same time, more optimistic conclusions have been drawn[8] on the lower bound of applicability of this approximation from extrapolations of the experimental Hugoniot adiabats. Recently a considerable number of theoretical[9,13,75,77] and experimental[10,11,23–25,76] studies have been devoted to finding the limits of applicability of the quantum-statistical models. Here considerable deviations have been established at pressures of hundreds of megabars from the traditional[7] quantum-statistical description, which completely ignores the electron shell structure of the elements. A detailed theoretical analysis[7,9,12] has established that the shell effects can be qualitatively described within the framework of the quasiclassical approximation by allowing for a correction nonanalytic in $\hbar$ that corresponds to the oscillating component of the electron density formerly omitted incorrectly. The essential point is that these effects are described already in the lowest quasiclassical approximation. Hence they should be taken into account along with the traditional regular corrections. The quasiclassical allowance for shell effects appreciably changes the equation of state of strongly compressed matter in the region $p > 300$ Mbar, leading to breaks in the atomic-volume curve[12] and lack of smoothness of the zero-point isotherms (Fig. 1) that corresponds to first-order phase transitions upon "squeezing out" the energy levels into a continuous spectrum.

Considerable deviations from the "average" behavior

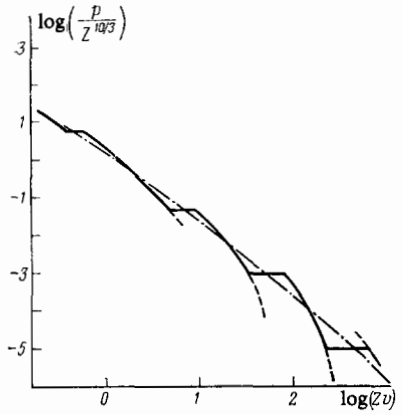

FIG. 1. The equation of state according to the quasiclassical model with shell effects taken into account according to Refs. 7 and 12.

of matter at tens or hundreds of Mbar are also indicated by the data of more exact quantum-mechanical calculations of the equation of state of aluminum by the Hartree-Fock-Slater method at temperatures of tens and hundreds of eV (Figs. 3 and 4). Interestingly, the nonmonotonicity of the thermodynamic quantities caused by shell effects is also predicted on the basis of quasichemical models of a plasma that allow for thermal ionization and pressure ionization[14] (Fig. 5).

Recently published experiments[10,11,76] on compression of condensed media by high-power shock waves apparently indicate deviations from the Thomas-Fermi model and an influence of shell effects at pressures of the order of 10 Mbar.[3,77]

Thus the problem of the lower bound of applicability of the quantum-statistical model remains open at present, while the behavior of matter in the multimegabar range of pressures is more complicated and varied than it had seemed before on the basis of simplified models.

The experimental techniques employed in high-pressure physics can be divided into two fundamental fields. Under static conditions, the use of especially strong diamond

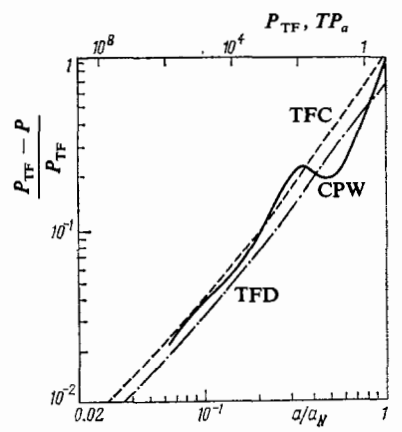

FIG. 2. The equation of state of aluminum according to the Thomas-Fermi-Dirac (TFD) model, the Thomas-Fermi model with quantum and exchange corrections (TFC), and the model of combined plane waves (CPW).[9] a is the lattice parameter, $a_N = 7.65\,a_0$; a_0 is the parameter under normal conditions.

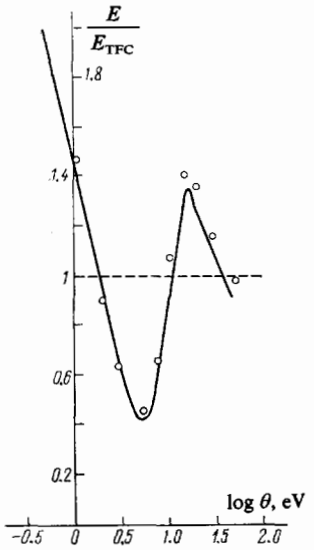

FIG. 3. Ratio of the magnitudes of the energies in the Hartree-Fock-Slater model[13] (HFS), the Thomas-Fermi model with quantum and exchange corrections (TFC), and in a "chemical" model of the plasma (dots) as a function of the temperature at a pressure of 1 kbar.[13]

anvils enables one to determine the isothermal compressibility, the electric conductivity, and optical spectra, and to perform detailed x-ray structural study of materials at pressures up to 1 Mbar.[15,16,79] The record-setting pressure values under controlled conditions have been attained at present by dynamic methods, which enable one to obtain states with high local concentrations of energy for a short ($\sim 10^{-6}$ s) time determined by the gasdynamic dispersal of the material being studied. Detonation of condensed explosives and also light-gas propellant apparatus make it possible to carry out detailed thermodynamic,[1] optical,[2] and electrophysical[17,19] measurments for a wide set of condensed media at character-

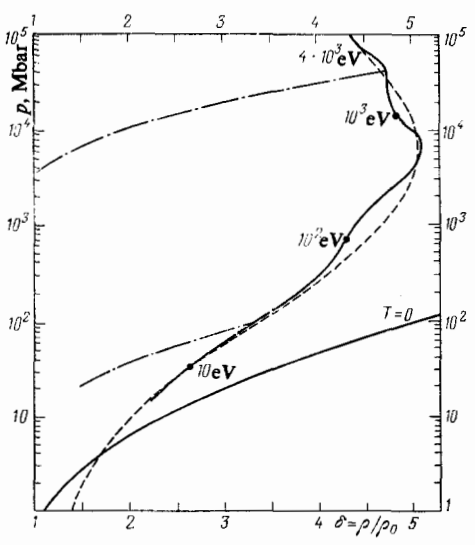

FIG. 4. Shock adiabat of iron,[75] $\rho_0 = 7.85$ g/cm^3, and the cold compression curve ($T_0 = 0$ K) with shell effects taken into account (solid curves). Dotted line: results of smooth joining of experiment and calculations by the Thomas-Fermi model with corrections. Dot-dash line: expansion isentropes.

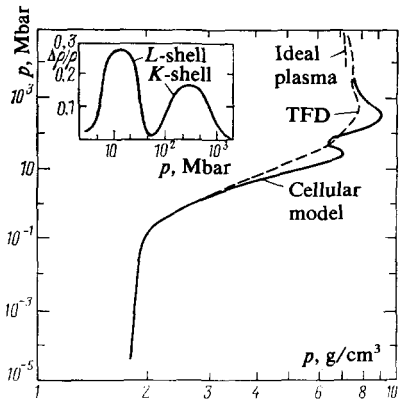

FIG. 5. Shock adiabat of solid beryllium.[60] Inset: relative density difference between the calculations by the cellular model and the Thomas-Fermi-Dirac model.

istic pressures up to 5 Mbar. The method of adiabatic expansion of shock-compressed metals[18] as well as the explosive compression of gases[19] yield information on the behavior of strongly nonideal Boltzmann and degenerate plasmas at pressures $p \lesssim 1$ Mbar.[3] Employment of explosive compression of a magnetic field enables one to find states on the compression isentropes at pressures up to 10 Mbar.[21,21,22] The current record-setting pressures of 10–100 Mbar have been obtained in the near zone of powerful explosions,[8,10,11,23–25,76,93] where relative (depending on the standard being used, the results vary within a range up to 50%[8]) and absolute measurements have been performed. However, even these record-setting pressures are still rather far from the lower bound of the quantum-statistical description.

A distinctive feature of the diagnostics in the dynamic measurements consists of the use of the general laws of conservation of mass, momentum, and energy to determine the caloric equation of state $E = E(p, V)$[5]:

$$\frac{V}{V_0} = \frac{D-u}{u}, \quad p = p_0 + \frac{Du}{V_0}, \quad E = E_0 + \frac{1}{2}(p+p_0)(V_0 - V). \tag{2.1}$$

The concrete measurements reduce to fixing distances and measuring the times which the shock waves and contact surfaces take to traverse these distances (baselines). This can be done with high accuracy. Comparison of the different models (Figs. 1–6) indicates that the characteristic difference between them in the pressure range > 10 Mbar can reach

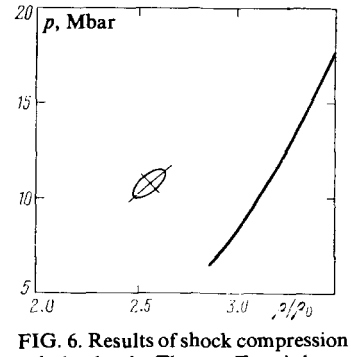

FIG. 6. Results of shock compression of aluminum[10]—ellipse; curve; calculation by the Thomas-Fermi theory with corrections.[12]

~ 30–50% in terms of pressure. In agreement with the following relationship, which stems from (2.1):

$$\frac{\Delta\rho}{\rho} = \left(\frac{\rho}{\rho_0} - 1\right)\sqrt{\left(\frac{\Delta D}{D}\right)^2 + \left(\frac{\Delta u}{u}\right)^2}$$

this requires a characteristic accuracy of measurement of the phase velocities D and the group velocities u of motion of the shock waves of no poorer than 5–10%. We note that this holds for single-phase situations. The appearance of phase transitions in a strongly compressed plasma[2,4] can qualitatively distort the portion of the phase diagram being studied by causing sharp jumps in the thermodynamic functions and hydrodynamic anomalies[80] of the type of multiwave structures and rarefaction shock waves.

It is essential to stress that specific conditions for the self-preserving nature of the flow[5] have to be satisified in order to be able to use the dynamic method of diagnostics according to the conservation laws in the algebraic form (2.1): the shock wave must be homogeneous and in a steady state, and the initial conditions ahead of its front must be known exactly.

Upon evaluating the situation as a whole, we see that the most accessible regions for a contemporary theoretical description are those of extreme pressures and temperatures, which occupy the periphery of the phase diagram of the material, whereas the most interesting inner part, intensively employed in applications, is accessible in the best case only to qualitative analysis. Here, over a very extensive region of the phase diagram, the construction of well-grounded physical models of matter is being impeded by the almost total lack of experiments requiring high local concentrations of energy.

3. POTENTIALITIES OF LASERS FOR GENERATING HIGH-POWER SHOCK WAVES IN CONDENSED MEDIA

a) Very simple estimates of the pressure in a plasma

Very simple estimates of the pressure attainable in steady-state laser irradiation can be carried out on the basis of a one-dimensional model,[26] according to which the flow field of the plasma is divided into three regions: 1) a steady-state shock wave, which is followed by 2) a Chapman-Jouguet wave, where the absorption of light energy occurs and flow is closed by 3) a simple centered rarefaction wave (which is adiabatic or isothermal). Under these approximations the following relationship holds for the pressure of a shock-compressed ideal ($\gamma = 5/3$) plasma:

$$p = \begin{cases} p_c & \text{when } t \leqslant t_1, \\ p_c\left(\frac{t_1}{t}\right)^{1/8} & \text{when } t > t_1. \end{cases} \tag{3.1}$$

Here $t_1 = 0.63\, I^{2/3}\beta^{-1}\rho_c^{-8/3}$ is the time at which the plasma corona begins to shield the target owing to deceleration absorption with the coefficient $\varkappa_b = \beta\rho^2 c_s^3$, where $c_s = \sqrt{5T/3M}$, and ρ_c is the critical density of the plasma ($\omega_0 = \omega_p = \sqrt{4\pi n_c e^2/m}$). In this case the maximum attainable pressure is[26,14]

$$p_c \approx I^{2/3}\rho_c^{1/3}. \tag{3.2}$$

The pressures calculated from these relationships for wave-

lengths of 10.6 μm, 1.06 μm, and 0.53 μm are shown in Fig. 7, which also shows the experimental date.[27,82,83,124] In the case in which an appreciable amount of light energy is absorbed in the corona with $n_e < n_c$ (regime with $t \sim t_1$), one can employ an isothermal instead of an adiabatic expansion wave to estimate the effect of the corresponding temperature increase on the parameters of the shock wave. According to Ref. 5, this diminishes the shock-wave pressure by 26%. On the other hand, one can estimate the upper bound of the possible pressures by assuming that all the energy of the incident light goes into maintaining the shock wave. In this approximation[26] we have

$$p_m = \left(\frac{\gamma+1}{2}\rho_0 I^2\right)^{1/3} \sim \frac{\rho_0}{\rho_c} p_c .$$

Upon analyzing the relationships (3.1) and (3.2) we see that the pressures attainable in the laser method of generating pressure depend weakly on the chemical composition of the target. This constitutes the essential difference of the methods of laser generation from the methods that have become classical in dynamic physics that use the impact of metallic plates or the products of detonation of condensed explosives.[1] Characteristically, high-frequency radiation possesses considerable advantages from the standpoint of obtaining maximal plasma pressures. However, as we shall see below, the fundamental advantage of short-wavelength radiation consists in the diminished effect of the nonthermal electrons with increasing laser frequency (see Sec. 4).

We should bear in mind the fact that the qualitative estimates given here have been obtained for an interval of parameters of the laser pulses in which the presented simplified model of the interaction process is doubly schematic. The point is that, at radiation intensities of the order of 10^{13}–10^{17} W/cm^2, the absorption of light is substantially nonlinear in character. Here a considerable part of the light is reflected from the plasma, and the reflection coefficient also depends on the intensity of the radiation. Consequently the formula for the absorption coefficient used to estimate the shielding time proves to be highly simplified. The screening model itself will be more complicated in this case, since at the focal-spot dimensions of practical interest we cannot consider the flow in the corona to be homogeneous. A further entire set of complications arises at high laser intensities that can be taken into account fully enough only within the framework of a complex numerical simulation (see, e.g., Ref. 34). Therefore we shall study below the fundamental physical processes that are taken into account in the contemporary schemes of numerical simulation, discuss the results of simulation and compare them with the simple estimates given above. We note further that, in view of the unwieldiness of the current programs for numerical simulation and the considerable degree of arbitrariness in the construction of physical models, simple estimates analogous to those of Ref. 25 retain a certain value even outside the limits of applicability of the initial assumptions.

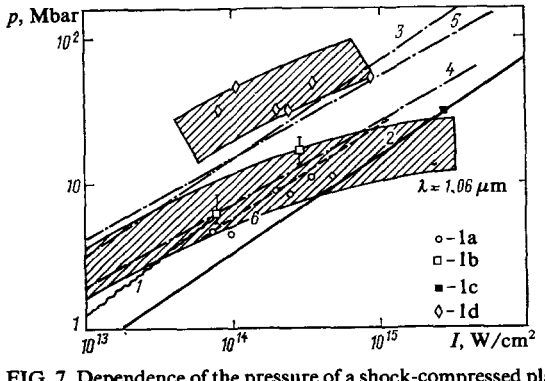

FIG. 7. Dependence of the pressure of a shock-compressed plasma on the intensity of laser radiation. Experiment: 1—[82]; 1*a*—[83]; 1*b*—[27]; 1*c*—[83]; 1*d*—[124]; 2—calculation by (3.2), $\lambda = 10.6$ μm; 3—calculation by (3.2), $\lambda = 1.06$ μm; 4—scaling of (3.6); 5—Eq. (3.6) with $\lambda = 0.35$ μm; 6—Eq. (3.4) with $\alpha = 0.65$. Crosshatched regions: experiments for $\lambda = 1.05$ and 0.53 μm.[84]

In proceeding to analyze the physics of the interaction of laser radiation with matter, we shall restrict the treatment only to a brief description of the fundamental processes. More detailed information is contained in the reviews of Refs. 31–33, 128, 148.

b) Absorption of laser radiation

Laser radiation incident on a target is absorbed in the plasma "corona"—the outer layer of plasma where the electron density does not exceed the critical value $n_c = m\omega_0^2/4\pi e^2$. It is defined by the equality of the frequency of the laser radiation to the local electronic plasma frequency $\omega_p = \sqrt{4\pi e^2 n_e/m}$. The surface at which the electron density becomes critical is reflective. The real component of the dielectric permittivity of the plasma $\mathrm{Re}\,\varepsilon(\omega)$ vanishes there. The integral absorptive power of the corona is determined by the spatial profile of the imaginary component of the dielectric permittivity.

In the approximation of geometrical optics,[129] the ratio of intensities of the reflected and incident radiation is

$$R = \exp\left(-2\int_{-\infty}^{x_0} \frac{\omega_p(x)\,\nu(x)\,dx}{c\omega_0^2\sqrt{1-(\omega_p^2(x)/\omega_0^2)}}\right).$$

Here x_0 is the coordinate of the point of reflection, and $\nu(x)$ is the effective frequency of collisions. The integrand is the absorption coefficient $\varkappa$ of light. It has a singularity at the reflection point x_0. Upon expanding $\omega_p(x)$ and $\nu(x)$ about this point, we obtain $R \approx \exp[-2\nu(x_0)L/c]$. Here $L = (d\ln n_e/dx)_{x_0}^{-1}$ is the spatial scale of the electron density near the reflection point (the corona is assumed to be isothermal). At moderate intensities of laser radiation, the quantity L is determined by the hydrodynamic expansion of the plasma in the corona. With increasing intensity, the light pressure, the recoil momentum of fast ("nonthermal") electrons, and other factors begin to affect the profile of electron density in the corona (see Refs. 128, 132, and 133).

When the energy flux density is not too large, the fundamental contribution to the effective frequency comes from the Coulomb collisions of electrons with ions. A calculation using the kinetic equation (see Refs. 47, 129, 130) leads to the following expression for the absorption coefficient:

$$\varkappa_b = \frac{16\pi}{3}\frac{\sqrt{2\pi}\,Zn_e^2e^6\ln\Lambda}{c\,(mT_e)^{3/2}\omega_0^2\sqrt{1-(n_e/n_c)}}. \qquad (3.3)$$

Here we have $\Lambda = \rho_D/b_{min}$, where ρ_D is the Debye radius,

and $b_{\min} = \max\{Ze^2/T_e, \hbar/\sqrt{mT_e}\}$. This formula has been derived under the assumption that the electrons obey a Maxwell distribution. Actually this is far from being always true. One of the mechanisms of breakdown of an equilibrium distribution of the electrons involves the fact that, in a plasma having the mean charge $Z > 1$, the frequency of electron-electron collisions that establish a Maxwell distribution is lower than the frequency of electron-ion collisions, which lead to absorption and which break down the equilibrium distribution. The resulting distortion of the electron distribution function leads to an appreciable decrease in absorption.[128] Another mechanism is even more obvious, and consists of the fact that an electron oscillates in the field of the electromagnetic wave, while moving with a velocity $v_E \sim eE/m\omega_0$, in addition to its thermal movement. At a high enough intensity of radiation, this velocity can become larger than the electron thermal velocity.[131] One can take the decline in the absorption coefficient into account approximately by multiplying Eq. (3.3) by the coefficient $[1 + (3v_E^2/2v_T^2)]^{-1}$.

The deceleration absorption declines with increasing electron temperature. Hence we could expect that the plasma will become ever more transparent with increasing intensity of the radiation. Actually the situation proves to be more complex, since at high intensities collective mechanisms of light absorption involving excitation of plasma waves begin to play a role. One of these mechanisms is resonance absorption. It consists of the excitation of Langmuir oscillations by the electric field of an incident electromagnetic wave having a component in the direction of the gradient of the electron density. The fraction of the radiation energy converted into plasma oscillations depends on the angle of incidence θ. At the maximum, where $\theta = \arcsin[0.8(\omega_0 L/c)^{1/3}]$, it amounts to about 60%.

The plasma waves excited in the case of resonance and other collective mechanisms of absorption decay by transferring their energy to electrons. The energy distribution of the electrons heated in this way depends on the mechanism of decay. As numerous theoretical and experimental studies show, it differs substantially from an equilibrium distribution. A numerical simulation of resonance absorption at high intensities of laser radiation (with the parameter $I\lambda_0^2 > 3\cdot 10^6$ W)[62] shows that a considerable fraction of the electrons is anomalously accelerated in the direction opposing the density gradient. The group of accelerated electrons has a distribution close to Maxwellian with the temperature

$$T_h \approx 7\,(T_e I\lambda_0^2)^{1/3}.$$

Here the laser intensity I is measured in units of 10^{15} W/cm^2, the wavelength λ in micrometers, and the temperature of the "thermal" electrons in keV. An experiment[63] performed under conditions in which resonance absorption plays the main role yields a similar dependence of the energy of the fast group of electrons on the laser intensity and frequency.

Another mechanism of generation of plasma waves in the corona is parametric excitation. Under the conditions characteristic of experiments with nanosecond pulses, two parametric processes are most important. They can be conveniently treated in terms of the decay of an initial electromagnetic wave (t) respectively into two Langmuir waves (l and l'): $t \to l + l'$, or into a Langmuir wave (l) and an ion-sonic wave (s): $t \to l + s$. Both decays have a laser-intensity threshold. For the two-plasmon decay this threshold is minimal at an electron density close to $n_c/4$, and for decay into a plasmon and a "phonon" at $n_e \approx n_c$. The threshold is determined by the damping of the waves formed by decay and depends on the electron-density gradient near the points n_c and $n_c/4$, respectively. At intensities exceeding the threshold, both parametric processes contribute to the effective frequency of collisions. An extensive literature has been devoted to calculating this contribution. A linear theory has been presented in detail in Refs. 32, 125, 126. When the threshold is considerably exceeded, the parametric instabilities have been studied by numerical methods.[64,134–139] The pattern established by simulation (effective frequencies of collisions, intensities and shapes of the lines of the harmonics $2\omega_0$ and $(3/2)\omega_0$) agrees qualitatively with experiment. However, definite caution is needed in employing the results of simulation in quantitative hydrodynamic calculations.

In addition to the decay processes pointed out above, which lead to light absorption, analogous scattering processes can occur, in which an electromagnetic wave arises instead of a Langmuir wave: $t \to t' + l$, $t \to t' + s$. The former process is analogous to two-plasmon decay and amounts to stimulated Raman scattering (SRS). The latter is stimulated Mandel'shtam-Brillouin scattering (SMBS). Both processes lead to energy losses. Experimental study shows that in typical irradition regimes the losses in SMBS are relatively small. This can involve several possible mechanisms of stabilization of SMBS: formation of a sharp electron-density gradient near n_c, nonlinear heating of the ions, and inhomogeneity of the plasma in the direction transverse to the laser beam.

There is somewhat less information on SRS. This scattering process occurs in a rarefied plasma when $n_e \leqslant n_c/4$, and competes near the surface $n_c/4$ with two-plasmon decay. Numerical simulation[140] shows that both processes make possible an intense "pumping" of the plasma waves with frequencies near $\omega_0/2$. The pressure $E^2/8\pi$ that arises here causes fluctuations in the density of the plasma that suppress the instability. Then the inhomogeneities relax, and the cycle is repeated. There is some uncertainty in a quantitative estimate of the role of scattering, partly involving the dependence of the scattering on the irradiation conditions: the intensity, pulse duration, and spectral width.

The decay processes of absorption and scattering give rise to fast electrons. We cannot view the problems of the spectrum, angular distribution, and other parameters of this group of electrons as being completely solved. Undoubtedly, the collapse of Langmuir waves plays a substantial role in the generation of fast elecrons.[141] This phenomenon consists of the spatial localization of intense long-wavelength Langmuir oscillations accompanied by formation of cavities—regions with lowered plasma density. The excess gas kinetic pressure outside the cavity is equilibrated by the pressure of the high-frequency electric field of the waves enclosed in the cavity. The collapse of the cavities gives rise to an increase in

the field and acceleration of the electrons that cross the cavity within a time of the order of an oscillation period. All this sequence of events can be seen well in a numerical experiment[142,163] that confirms the concept of a collapse. However, it will take further study to obtain quantitative information on the fast electrons.

Yet another mechanism of absorption amounts to conversion of electromagnetic waves into plasma waves by intense ion-sonic turbulence. The excitation of surface oscillations by the density jump near $n_e = n_c$ at high laser intensities leads to the same effect.

Absorption and scattering of laser radiation in a plasma has been studied in detail experimentally. Without taking up the numerous original studies, we note that, for short pulses (< 1 ns) with an intensity $\sim 10^{15}$ W/cm^2 and $\lambda_0 = 1\,\mu$m with normal incidence on a plane target, the absorbed fraction of the radiation amounts to about 30% and depends weakly on the parameters of the pulse and of the target material.[143] The situation is more complicated in the case of long pulses of lower intensity. Here the data of different authors diverge appreciably, and one observes a dependence of the absorptivity on the fine structure of the laser pulse, the magnitude of the contrast, etc. For plane targets of medium Z in long pulses, about 80–90% of the incident energy is absorbed, so that in this case the only problem of practical importance is the distribution of the absorbed energy between the thermal and the fast electrons.

c) Energy transport by electron heat conduction

The radiation energy absorbed in the corona is transferred to the denser plasma by electron heat conduction. If the mean free path of an electron is small in comparison with the characteristic scale of the temperature distribution, the energy flux is given by the well-known formula[127]

$$q_T = -\chi(T_e)\nabla T_e, \quad \chi(T_e) = \frac{300T_e^{5/2}}{Z\ln\Lambda}\ (\text{W/cm}^2\cdot\text{eV}).$$

The actual region of applicability of this formula to a laser plasma is rather restricted. The point is that the heat flux cannot in any case exceed the energy flux transported by the plasma in free expansion into a vacuum $q_v \sim n_e v_T T_e$.[1)] Actually the restriction of the heat flux proves to be more severe. Among the factors restricting the heat flux, the most important are ion-sonic turbulence and spontaneous quasistationary magnetic fields. For a phenomenological description of the electron heat conduction under such conditions, one usually introduces the limiting flux $q_m = fq_v$, where the coefficient $f < 1$ is determined experimentally or is estimated from some particular transport model. Upon equating the absorbed energy flux $AI = (1 - R)I$ to the value q_m at the critical surface, we can obtain an estimate of the electron temperature of the plasma:

$$T_e \approx 3\left(\frac{A}{f} I\lambda_0^2\right)^{2/3}.$$

As above, we have adopted here the unit of 10^{15} W/cm^2 for I, λ_0 is measured in μm, and the temperature in keV. We see that the overheating of the corona decreases and the hydrodynamic efficiency increases with increasing frequency of the laser radiation.

The problem of electron heat conduction under conditions of strongly restricted flux ($f \ll 1$) has been studied experimentally[65,144–147] and theoretically.[66,149] It has been shown[66] that the restriction of the electron heat flux from ion-sonic turbulence leads to values of f lying in the interval $(m/M)^{1/4} > f > m/M)^{1/2}$. The complex pattern has been studied[149] of restriction of heat flux under the action of random quasistationary magnetic fields and also certain bounds were indicated for the factor f. We should stress that the description of the complex process of transport in an inhomogeneous plasma by fixing a single number f is, of course, an extreme approximation. Actually there are several competing mechanisms of energy transport (thermal electrons, fast electrons, ions, radiation, etc.), whose relative role depends on the parameters of the plasma. Nevertheless, one traditionally employs the following procedure in the experimental study of energy transport (see, e.g., Refs. 65 and 102). One performs a series of hydrodynamic calculations with different values of the parameter f, and then compares the results with experiment to find the most suitable value of f. Understandably, in such an approach it is hard to expect agreement between the results of experiments performed under differing conditions. The values of f given by different authors are scattered over about two orders of magnitude. The attempts to estimate the degree to which the energy transport by fast electrons is suppressed also have not yet yielded an unequivocal result (see, e.g., Refs. 145 and 146).

Thus, there is considerable uncertainty in the problem of electron energy transport. It affects to a greater extent the interpretation of experiments with long-wavelength lasers, since for them the spatial region in which the decisive process is energy transport by electrons is relatively large.

d) Hydrodynamic instability of plasma compression

The high pressures in a condensed phase under laser irradiation are created by the recoil momentum of the dispersing less dense material. The contribution of light pressure is small in most cases. The energy needed to heat and ionize the dispersing material is transmitted from the absorption zone by heat conduction. Owing to the nonlinear character of heat conduction, the heat wave has a sharp front in the small neighborhood of which the density of matter varies almost discontinuously, while the mass velocity changes sign. This region is called the ablation surface. At the onset of the laser pulse, when the radiation intensity is increasing with time, the ablation surface is accelerated in the direction of the density gradient. Such an acceleration in the coordinate system associated with the ablation surface is equivalent to a gravitational force directed from the denser layer of matter to the less dense. Consequently the ablation surface proves to be unstable.[32,150] Instability of this type is well known in hydrodynamics and is called Taylor instability.[151] One can find examples of study of instability under conditions of laser experiments in Refs. 30, 32, 150, 152, and 153. We shall present here a qualitative picture of the evolution of Taylor perturbations.

The linear increment of instability is $\gamma = \sqrt{|a|k}$, where

[1)] The two fluxes become equal when the spatial scale of the temperature distribution becomes of the order of the mean free path of an electron.

$|a|$ is the modulus of the acceleration and $k = 2\pi/\lambda$ is the wave number of the perturbation. On the short-wavelength side, the spectrum of growing perturbations is bounded by the quantity d, the characteristic scale of the density gradient at the ablation surface. The amplitude of small perturbations increases exponentially with time. After it has become of the order of the wavelength, the nonlinear stage of evolution of the perturbations sets in. "Bubbles" of the light component are formed, which "float up" in the dense layer with the constant velocity $v_\lambda = \mathrm{Fr}\sqrt{|a|\lambda}$, where Fr is the Froude number, with narrow "jets" of the heavy component, that "fall" with acceleration through the light layer. One can easily understand that, if the velocity of displacement of the ablation surface is $v_a > v_\lambda$, the "bubbles" with the corresponding wavelength will be broken upon interacting with the heat wave. Thus, the short-wavelength perturbations with $\lambda < \lambda_c$ will be suppressed owing to the movement of the ablation surface. Here we have

$$\lambda_c \approx \mathrm{Fr}^{-2}\left(\frac{v_a^2}{|a|}\right), \qquad \mathrm{Fr} \sim 0.2-0.4.$$

One can relate the critical wavelength λ_c to the scale d of the density at the ablation surface[30]: $\lambda_c \sim 10 d\, \mathrm{M_a}$, where $\mathrm{M_a}$ is the Mach number of the ablation surface. Perturbations with $\lambda > \lambda_c$ are not stabilized by ablation, and their growth can affect the structure of the flow behind the shock wave.

If the time of acceleration is large enough, the spectrum of the unstable modes is expanded. This is called turbulent mixing.[154–156] In numerical calculations of the compression, this process is described by introducing the phenomenological coefficients of "turbulent" transport.

The role of Taylor instability increases in the presence of perturbations with an appropriate wavelength in the laser beam or the irradiated target. We should stress that inhomogeneous irradiation becomes more deleterious with increasing frequency of the laser radiation. The point is that the critical density $n_c \sim \omega_0^2$ increases with increasing ω_0, and the absorption zone approaches the ablation surface. Here the temperature perturbation caused by inhomogeneous irradiation can affect the local velocity of ablation by breaking the symmetry of flow.

e) Numerical calculations and scaling relationships for the pressure of a shock-compressed plasma

One can obtain the most complete information on the behavior of a laser plasma under the conditions of concrete experiments from numerical calculations. A series of programs has been written for performing these calculations. They are based on a hydrodynamic description of the plasma in a one-dimensional, plane two-dimensional, or spherical geometry. To varying degrees of completeness, the numerical models take into account the processes briefly studied above of light absorption, energy transport, generation of fast electrons, and electron-ion relaxation. The more complex programs use a multigroup approximation to describe the transport processes. One can obtain some information on the programs applied for numerical simulation of a laser plasma from Refs. 34, 67–69, and 81.

The experience with numerical calculations shows that the differences in the physical models on which the programs are based appreciably affect the obtained results. Therefore the dependence of the pressure behind the shock wave on the intensity and frequency of the laser radiation as found from numerical calculations is not completely unequivocal. One can conveniently, write the "scaling" for the maximum pressure in the form

$$p_m = a I^\alpha \lambda_0^{-\beta}, \tag{3.4}$$

by determining the values of the exponents α and β from numerical or real experiments. Let us examine some examples.

The following relationship has been obtained from calculations on a one-dimensional variant of the program[34] for an aluminum target and a neodymium-glass laser (p in Mbar, I in units of 10^{15} W/cm^2):

$$p_m \approx 57\ I^{0.82}. \tag{3.5}$$

A calculation by the program of Ref. 67 also gives a power-function law for p_m but with the exponent 0.36. A numerical calculation and an analytic model[70] yield a relationship differing from a power function, with the absolute values of the pressure somewhat lower than those given by Eq. (3.5). An approximate interpolation of these results has the form

$$p_m \approx 27\ I^{0.57}. \tag{3.6}$$

A value $\alpha = 0.57$ of the exponent also arises from the experimental data obtained in Ref. 147. The pressure was determined from the velocity of dispersal with use of both the data of high-speed photography and the results of calorimetric measurements. The absolute value of the pressure obtained in experiments with an iodine laser ($\lambda_0 = 1.3$ μm) amounted to 300 kbar at $I = 2.5\times 10^{11}$ W/cm^2 and 50 Mbar at $I = 2\times 10^{15}$ W/cm^2.[2)]

Measurements were performed in Ref. 82 of the recoil momentum and the energy of the ions of the dispersed plasma that make possible a calculation of the mean pressure in the target for $I \leqslant 10^{14}$ W/cm^2. A description of the results of these experiments by Eq. (3.4) yields the value $\alpha = 0.8$.[83] According to the data of Refs. 83 and 84, the exponent α monotonically decreases with increasing radiation intensity. In the range 10^{14}–$3\cdot 10^{15}$ W/cm^2, the best description of the experimental data is attained with $\alpha = 0.6$.[83] The value $\alpha = 0.67$ was obtained[87] for intensities of the order of 10^{14} W/cm^2.

The information is less definite on the dependence of the pressure on the frequency of the laser radiation. A very simple analysis (see (3.2)) yields a value of the exponent $\beta = 0.67$, whereas a more rigorous treatment yields values of β from 0.33 to 2.0, depending on the adopted model of absorption.[83] The value $\beta \approx 1$ was obtained[85] from a detailed analysis for the spherical case, which, however, can deviate considerably from the solution of the plane problem.[86] Experiments[83] on generation of shock waves by the radiation of the third harmonic of a neodymium laser with $I \sim (1\text{–}2)\cdot 10^{14}$ W/cm^2 indicate an absorption of $\sim 95\%$ of the radiation incident on the plasma and yield a value of the exponent β close to 2/3, which agrees with the estimate of (3.2).

[2)]Reference 147 treats the dependence of the pressure on the *absorbed* laser intensity.

We note that, in the practical application of the scaling relationships (3.4)–(3.6) to regimes with high power and a considerable duration of the laser pulse, one should allow for the decrease in the radiation intensity caused by the two-dimensional dispersal of the plasma corona.[87]

The considerable ambiguity in the dependence of the pressure behind the shock wave on the parameters of the laser pulse indicates a present need of performing systematic calculations for determining the scaling laws for the intensity, frequency, atomic number, focusing area and other parameters of the experiment.

The results of using the "scaling" of (3.2), (3.4), and (3.6) to estimate the pressure in an aluminum target are shown in Fig. 7. The amplitude values of the pressures in the plasma of othe chemical elements as calculated by the program LASNEX[34] are presented in Fig. 8.[14] We see that one must operate with radiation intensities exceeding 10^{14}–10^{15} W/cm^2 in order to advance into the currently unstudied range of plasma pressures greater than 10 Mbar.

4. STRUCTURE OF LASER SHOCK WAVES AND GENERAL REQUIREMENTS ON THE DESIGN OF TARGETS

In this section we shall treat the requirements on the laser radiation and the dimensions of the targets necessary for obtaining in the studied material plane stationary and "thin" shock discontinuities propagating in the relatively cold material. This enables one to use the dynamic method of diagnostics based on the relationships (2.1). The restrictions that arise here determine the level of maximum pressures attainable with the aid of contemporary lasers.

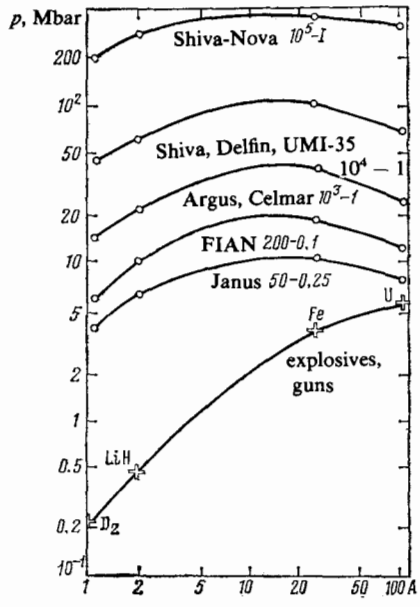

FIG. 8. Amplitudes of shock waves[14] generated by different laser systems based on neodymium glass. First number: energy in joules; second number: duration of pulse in nanoseconds. The lower curve characterizes the potentialities of the technique of chemical explosives and light-gas guns. A is the atomic number of the studied element.

a) Damping effects in the lateral and rear unloading waves

The first requirement typical of all dynamic experiments[1] consists in eliminating the influence of the lateral rarefaction waves (Fig. 9), which in propagating from the outer edge of the irradiated region toward the symmetry axis diminish the pressure and temperature of the shock-compressed plasma, and bend the front of the shock wave, which in the limit tends to become spherical.[35] The "head" of the lateral rarefraction wave propagates toward the axis with the velocity of sound in the shock-compressed plasma c_s, which is comparable with the phase velocity D of the shock wave (see Fig. 9). This means that if one must have a plane region of the shock front with a characteristic dimension R_g after passing through the target, then the dimension of the focal spot must be no smaller than

$$R_0 \geqslant R_g + d. \tag{4.1}$$

As a rule, in experiments with shock waves this condition is considerably strengthened: $R_0 \geqslant 10d$.[1] In view of the fact that electron heating requires the thickness of the target to be no smaller than tens of micrometers, the needed dimensions of the focal spot prove to be of the order of hundreds of micrometers. Upon considering that the laser radiation can be focused onto a spot of considerably smaller size ($\sim$ten micrometers), we can easily understand that this restriction is substantial, since the intensity is decreased by defocusing, and hence also the maximum plasma pressure is decreased. Moreover, it is desirable to have the laser radiation uniformly distributed over the area of the focal spot. Usually[14] this distribution has the form $I = I_0 \exp[r/r_0)^n]$ with n of the order of several units, with local inhomogeneities ("hot" spots) superimposed on the main profile. In addition to the inhomogeneities, which arise from defects of the laser and the focusing system, one can expect at high intensities additional distortions involving self-focusing and filamentation of the laser beam in the plasma. The effects of inhomogeneity are partially smoothed out by the electron heat conduction, so that the energy flux to the ablation surface essential for the hydrodynamic movement has far smaller space and time fluctuations than does the energy release near the critical surface. The studies of Refs. 82, 166 are devoted to the problems of the influence of inhomogeneity of irradiation on the hydrodynamics.

Figure 10 illustrates the damping of the shock wave caused by arrival of the rear unloading wave. At the instant τ that the laser irradiation ceases, an unloading wave sepa-

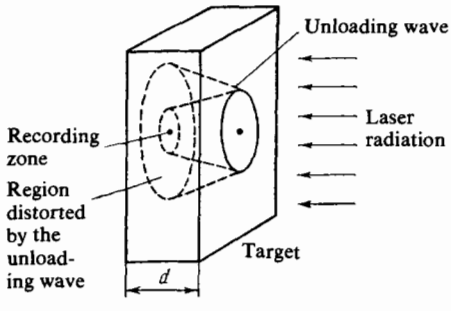

FIG. 9. Spatial diagram of flow in a target caused by laser irradiation.[39]

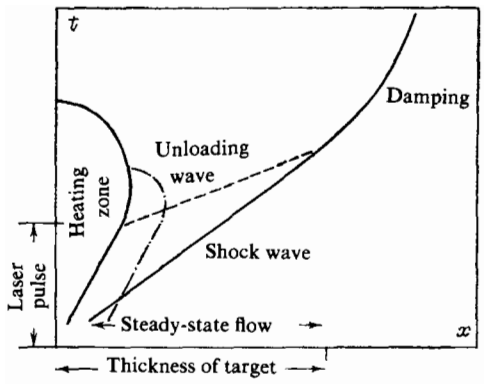

FIG. 10. Diagram of flow in laser generation of shock waves. Dot-dash line: zone of heating by nonthermal electrons.

rates from the absorption zone, and its "head" propagates with the velocity of sound $u + c_s$ through the shock-compressed plasma. Hence at the instant t_1 it overtakes the front of the shock wave, which from this instant begins to decrease in velocity. Upon assigning the Hugoniot adiabatic in the form $D = c_s + 1.5\,u$,[36] we can easily obtain the restriction on the baseline of measurement:

$$d \lesssim 2D\tau. \tag{4.2}$$

For a fixed value of d, this condition determines the minimum duration of the pulse that guarantees stationary flow of the plasma in the zone of measurements. For values of d of tens of micrometers ($D \sim 30$ μm/ns), τ proves to be of the order of 1 ns. Thus, beginning at these times, an increase in the intensity I can be effected only by increasing the energy of the laser radiation, rather than by shortening the duration of the laser pulse. Naturally, one must have a steady-state laser flux of high contrast for creating steady-state shock waves. However, even in this case deviation from a steady state can occur in the absorption zone of the type of instabilities of the critical surface and other effects.[37]

b) The effect of two-dimensionality of the dispersal of the plasma corona

At considerable intensities and durations of the laser pulse, differences arise in the flow of the plasma from a simple one-dimensional regime, even in the situation in which lateral and rear unloading waves are absent.[87] Figure 11 shows a diagram of the plasma flow. We see that for focused laser radiation (with a focusing angle θ), the area s of the critical surface on which the laser radiation is incident differs from the initial area s_0 of the spot on the surface of the target by the factor $[1 + (l_{AC}/R_s)\sin\theta]^2$, where $l_{AC}(I, t)$ is the characteristic distance from the ablation surface to the critical surface. Therefore the radiation intensity that enters into the relationships (3.8) and (3.4) depends on the maximum power W and the pulse duration τ (via the $l_{AC}(W, \tau)$ relationship). The expansion of the absorption region decreases the pressure of the plasma as compared with a regime of one-dimensional dispersal. The distance l_{AC} can be estimated in order of magnitude as being the product of the pulse duration times the velocity of sound in the plasma. This leads to the scaling

$$l_{AC} \approx l_{AC}^{(0)} \tau^{\delta} I^{\varepsilon}.$$

One can assume[87] that $\delta = 0.9$, $\varepsilon = 0.3$ on the basis of hydrodynamic calculations, which leads to a change in Eq. (3.4):

$$p_s = aI^{\alpha}\left(1 + \frac{l_{AC}^{(0)}}{R_s}\tau^{0,9} I^{0,3}\sin\theta\right)^{-2\alpha}. \tag{4.3}$$

Figure 12 compares the one- and two-dimensional regimes of flow for an aluminum target with $R_s = 256\,\mu$m and thickness 72 μm when irradiated with a laser pulse at $\lambda_0 = 1.06$ μm of Gaussian shape with a focusing angle $\theta = 22°$.[87] For the same focusing conditions, Fig. 13 indicates[87] the parameters of the laser pulse for which the difference between the two- and one-dimensional calculations does not exceed an assigned value.

We stress that our remarks pertain to the nonuniform dispersal of the rarefied plasma in the corona near the critical surface. In the dense plasma near the ablation surface the temperature is lower. Hence the effects of two-dimensionality for movement of the shock wave and flow of the plasma behind it need not be so essential. For example, under the conditions of the experiments of Ref. 83, the regime of shock compression of the target material proves to be one-dimensional (within the limits of accuracy of the measurements).

c) Formation of a quasistationary shock wave

In the laser irradiation of a target, the shock wave is not formed instantaneously, but after a certain time τ_s and at a cerain distance l_s from the surface. The process of formation of the shock wave imposes certain restrictions on the choice of target parameters. Let us examine this problem in greater detail. For simplicity we shall restrict the treatment to the

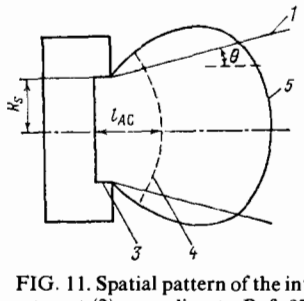

FIG. 11. Spatial pattern of the interaction of a focused laser beam (1) with a target (2) according to Ref. 87. 3—ablation front; 4—critical-density surface; 5—plasma corona.

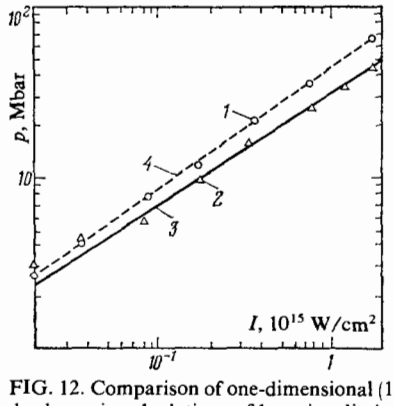

FIG. 12. Comparison of one-dimensional (1) and two-dimensional (2) hydrodynamic calculations of laser irradiation of aluminum targets.[87] 3—calculation by Eq. (3.4) with $a = 8.0$, $\alpha = 0.7$; 4—calculation by the model (4.3).

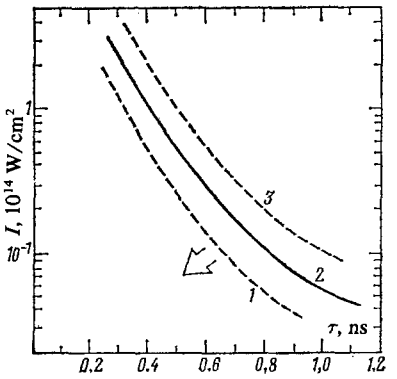

FIG. 13. Parameters of laser pulses for which one must allow for the two-dimensionality of dispersal of the plasma corona.[87] 1–3—boundaries of the regions of parameters where the difference between the two- and one-dimensional calculations does not exceed 8, 10, and 12%.

one-dimensional case. Laser radiation incident on a target heats the electrons. Transfer of energy to ions occurs relatively slowly, owing to the large mass difference. Therefore mass movement is absent in the initial stage of action of the laser pulse, while the energy is transported from the absorption site by electron heat conduction. The heat wave propagates according to the law

$$x_T \sim \sqrt{\frac{\chi t}{nk}} \sim v_T \sqrt{\tau_{tr} t}.$$

Here V_T is the thermal velocity of the electrons and τ_{tr} is the transport time.[127] The gradient of electron pressure leads to motion of the matter. The hydrodynamic perturbation propagates according to the law

$$x_s \sim c_s t \sim \sqrt{\frac{m}{M}} v_T t.$$

We are interested in the case in which the shock wave propagates through cold matter, while the presonic heat wave plays the role of a "piston." One can obtain an estimate for the time τ_s for establishment of this regime from the condition $x_s = x_T$. We can easily see that $\tau_s \sim (m/M)\tau_{tr} \sim \tau_{ei}$. The thickness of the layer in which the shock wave is formed is equal in order of magnitude to $l_s \sim c_s \tau_{ei} \sim l_e \sqrt{M/m}$, where l_e is the mean free path of an electron at the instant of detachment of the shock wave from the layer heated by electron heat conduction ($x_s \approx x_T$). The temperature of the electrons at the instant of detachment is determined by the total energy E_s absorbed up to this time, and is equal to $T_s \sim E_s/nkl_s$. The problem of the transition from the heat-wave regime to hydrodynamic motion has been treated in Ref. 71. Here we shall give only a very simple estimate. At a constant laser intensity we have $E(t) = E_0 t/\tau$, where E_0 is the total energy and τ is the duration of the pulse. If we assume for the sake of definiteness that $n_i = 6\times 10^{22}$ cm^{-3}, $Z = 3$, and $M = 27\,M_n$, and carry out simple calculations, we obtain $\tau_s = 10^{-24}\,If(c)$ and $l_s = 5\cdot 10^{-23} I^{4/3} f$ (cm), where $I = E_0/\tau$ is the intensity of the laser radiation in W/cm^2. A certain indefiniteness in the time and the spatial scale of formation of the shock wave involves the fact that we do not know the factor f that takes into account the restriction on the heat flux. Apparently the restriction is inessential at an intensity $\sim 10^{13}$ W/cm^2, and l_s proves to be of the order of 0.1 μm.

In the intensity region $I \sim 10^{15}$–10^{16} W/cm^2, the factor f is of the order of 10^{-2}. Hence we should expect values $l_s \sim 1$–10 μm. The thickness of the targets must be much greater than l_s. In the case of high radiation intensity, this may be hard to fulfill, owing to the rapid growth of the laser energy with increasing thickness of the target.

The estimate that we have given was derived under the assumption that the duration τ of the laser pulse is in any case not smaller than the time τ_s for establishment of hydrodynamic motion. At constant laser intensity, such a regime corresponds to a shock wave of constant amplitude (the analysis in Ref. 26, which was presented at the beginning of Sec. 3, is based precisely on the scheme of such a flow). The laser energy needed to establish such a regime increases very rapidly with increasing shock-wave pressure. In principle a more "economical" regime is possible, in which the duration τ of the laser pulse is much shorter than the time τ_s. An estimate analogous to that presented above gives the following values in this case for the time and the path length of formation of the shock wave: $l_s \approx 10^{-6} E_0^{2/3} f$ (cm), $\tau_s \approx 2\cdot 10^{-12} E_0^{1/2} f$, where E_0 is the absorbed energy (in J/cm^2). The condtion $\tau \ll \tau_s$ can be written in equivalent form as $E_0 \tau^{-2} \gg 3\cdot 10^{23}$ J/cm^{2}s^2. The mass movement of the medium when $\tau \gg \tau_s$ is described in this case by the model of a "brief" shock.[71] The amplitude of the pressure in the shock wave decreases with time (approximately as $t^{-2/3}$ in the plane case), owing to the increase in the mass of the material brought into motion. A quantitative interpretation of experiments with brief laser pulses requries detailed numerical calculations of the plasma movement that arises.

d) Heating of the target by nonthermal electrons

The most serious restrictions on the parameters of targets are imposed by the requirement of eliminating the heating of the material ahead of the shock wave by the nonthermal (fast) electrons generated in the corona by the process of anomalous absorption. These electrons have an energy of 2–200 keV (depending on the laser intensity; see Sec. 3) and they give rise to almost instantaneous uniform overheating of a surface layer of the target of thickness comparable with their mean free path. The preliminary heating alters the initial state of the medium ahead of the shock wave. If this change is appreciable, then, in addition to measuring the two parameters characterizing the propagation of the shock wave, one must measure the initial state of the target. If we assume that the fast electrons cause only a growth in the initial energy (temperature) ΔE_h of the target, one can derive the following formula for the corresponding variation of ΔE of the energy of the shock-compressed plasma[39]:

$$\frac{\Delta E}{\Delta E_h} = \left[2 + \frac{\partial p}{\partial E}\left(\frac{1}{\rho_0} - \frac{1}{\rho}\right)\right]\left[2 + \frac{(p_s + p_0)\,\partial p/\partial E}{\rho^2\,\partial p/\partial \rho}\right]^{-1} \equiv \Sigma.$$

The calculations show that Σ varies over the range 1.5–2, depending on the concrete equation of state. Figures 14–17 show the results of calculating the characteristics of a shock-compressed plasma described by one of the variants of the quasiclassical theory[7,8] as a function of the pressure behind the shock wave. For expected temperatures of the compressed material $\sim$10–100 eV (see Fig. 16), the admissible

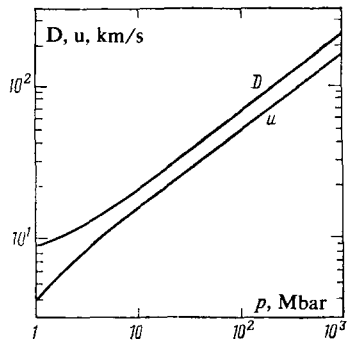

FIG. 14. The phase velocity D and the group velocity u of shock waves in aluminum as calculated by the quasiclasssical theory (TFC).[7,8]

temperatures of preheating must not exceed 0.1–1 eV.

The following expresison has been derived[72] by processing of numerical calculations to give the energy of the fast electrons formed in resonance absorption:

$$T_h \approx 8T_e^{0.25}(I\lambda_0^2)^{0.39}. \quad (4.4)$$

Here T_h and T_e are the temperatures of the fast and the thermal electrons in keV, I is in units of 10^{15} W/cm^2, and λ_0 is in μm. A similar relationship has been derived in Ref. 62 (see Sec. 3). We note that the temperature T_h is anisotropic: the electrons are acclerated mainly in a direction opposite to the density gradient. The depth of penetration of the fast electrons can be estimated by the formla

$$R_h \approx \frac{3\cdot 10^{18}T_h^2}{Zn_e} \text{ (cm)}. \quad (4.5)$$

(In this formula T_h is in keV.) If we assume, in line with model of Refs. 7 and 8, that $n_e = 6\cdot 10^{23}$ cm^{-3}, and $Z = 3$ for shock-compressed aluminum at 10-Mbar pressure, we obtain the estimate[3)] $R_h \approx 2\times 10^{-6}T_h^2$. More complete data on the mean free path of fast electrons in aluminum compressed by shock waves caused by laser radiation of varying frequency and intensity are given in Table I. The pressure behind the shock wave has been calculated from the model of Ref. 70, the electron density and the mean charge according to Refs. 7 and 8, and the energy of the fast electrons according to Refs. 62 and 72. The depth of heating, and hence the necessary target thickness, rapidly increase with increasing intensity of the laser radiation, but they decrease with increasing frequency. The frequency dependence of the depth of heating, in particular, makes it not very promising to employ CO_2 lasers to generate strong shock waves in condensed media.

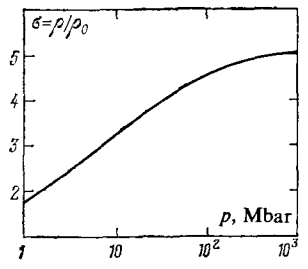

FIG. 15. Degree of compression of aluminum in a shock wave according to the quasiclassical theory.[8,7]

[3)]Of course, under these conditions one cannot consider compressed aluminum to be a weakly nonideal plasma for which Eq. (4.5) holds. Hence the magnitudes of the mean free paths given below amount to estimates.

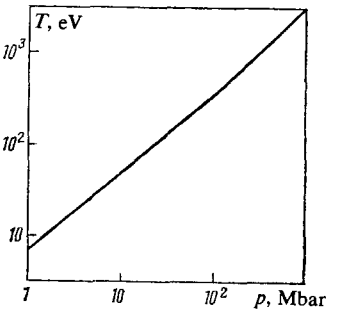

FIG. 16. Temperature of a shock-compressed plasma according to TFC.

A quantitative account of the effects of heating (see Sec. 5) shows that, in order to eliminate the distorting effect of nonthermal electrons, at $I\sim 10^{14}$–10^{15} W/cm^2 one must choose dimensions of the target $d\geqslant 20\,\mu$m. However, the preliminary results of experiments[41] apparently show the observed heating effect to be severalfold smaller than is expected. According to the data of Ref. 83, a change in the wavelength of the laser radiation from 1.06 μm to 0.53 μm at an intensity of $3\cdot 10^{14}$ W/cm^2 reduces the temperature of an aluminum target heated by fast electrons from several thousand degrees to negligibly small values.

Owing to the extreme complexity of the quantitative description of the role of nonthermal electrons, it seems expedient to perform a series of special experiments by varying the intensity and wavelength of the radiation, and also the dimensions d of the target.

Under the condition $d\sim R_h$, we note that a profile of the initial temperature $T_0 = T_0(x)$ is realized owing to electron heating that leads to inhomogeneity of the parameters in the shock-compressed plasma. At considerable radiation intensities in thick targets one can expect generation of secondary shock waves arising from the region of electron heating and moving ahead of the main shock wave.[98]

The x-radiation from the plasma can play a definite role in the preliminary heating of the material ahead of the front of the shock wave. The experimental data on this problem are equivocal. Estimates show that heating by radiation is less deleterious than heating by fast electrons. This conclu-

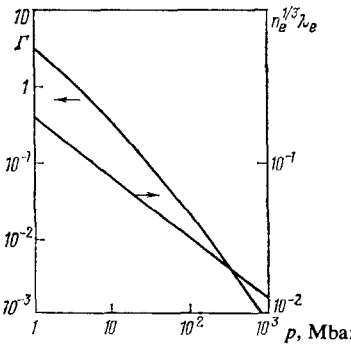

FIG. 17. The nonideality parameter $\Gamma = \sqrt{8\pi n_e}e^3/T^{3/2}$ and the degeneracy parameter $n^{1/3}\lambda_e$ of an aluminum plasma.

TABLE I. Mean free path of electrons in aluminum compressed by shock waves created by laser radiation (wavelength in μm).

I, W/cm^2	T_h, keV				R_h, μm			
	10.6	1.06	0.53	0.26	10.6	10.6	0.53	0.26
10^{14}	36	2,8	1,3	0,6	35	0,16	0,017	0,0050
10^{15}	130	10	4,6	2,1	340	1,3	0,29	0,055
10^{16}	460	36	17	7,7	2 800	16	3,5	0,68
10^{17}	1700	130	60	28	36 000	200	42	9,0

sion is confirmed by numerical calculations.[39] However, a complete and well-grounded answer to the question of the effect of radiation heating requires further study.

e) Scaling relationships for homogeneous targets

Now let us estimate how the laser energy required to attain a given pressure in the target depends on the value p of this pressure and on the wavelength λ_0 of the radiation. Evidently the energy is $E \sim IR_0^2\tau$, where R_0 is the dimension of the focusing spot on the surface of the target. We shall find the pulse duration τ from the condition (4.2): $\tau \geqslant d/2D$. The target thickness d must be much greater than the depth of heating R_h of the fast electrons, to estimate which we use Eq. (4.5). As regards the dimension of the focal spot R_0, its minimum size is determined by the absence of damping from the lateral unloading waves. Hence we can take R_0 as proportional to the thickness d of the target. Thus we have

$$E_{las} \sim I d^3 D^{-1} \sim I R_h^3 p^{-1/2}.$$

Upon using Eq. (3.2) to estimate the pressure and Eq. (4.4) for the energy of the nonthermal electrons, we obtain the following similarity relationship for the total energy of the laser radiation.

$$E_{las} \sim p^6 \lambda_0^{11}. \tag{4.6}$$

The exponents in (4.6) are highly sensitive of the details of the procedure adopted for estimating E and to the values of the exponents in the approximate formulas for the pressure, the electron temperature, and the energy of the fast electrons. However, in all the physically reasonable variants of the estimate, the laser energy increases very rapidly with increasing pressure and wavelength. Importantly, this conclusion pertains to the very simple method of generating plane stationary shock waves in homogeneous targets, where the fundamental physical restriction is the heating by the nonthermal electrons. Since the modern high-power laser systems already amount to gigantic engineering projects, it is unlikely that further increase in laser energy will be gained by increasing the geometric dimensions. Therefore a constructive way of moving up in the pressure scale of laser shock waves is to decrease the wavelength and to employ layered targets that diminish the role of electron heating.[39]

In addition to the evident potentialities of using short-wavelength lasers (e.g., KrF, XeF, H_2, etc.), one can obtain high-frequency radiation at high power by doubling the frequency of the radiation of a neodymium laser and its harmonics. Considerable advances have been made in recent years along this line. The nonlinear KDP crystal is very effective in the visible and near infrared regions for frequency doubling. It has been reported[74] tht an efficiency of second-harmonic conversion of the neodymium laser (0.53 μm) of more than 50% has been attained and an efficiency of more than 15% of conversion into the fourth harmonic (0.26 μm) has been reached at an energy level of 20 J in 100 ps or 100 J in 2.5 ns at 1.06 μm (this corresponds to 11 J in 75 ps and 35 J in 2 ns at 0.53 μm, and 3 J in 60 ps at 0.26 μm). Reports have been published very recently on an efficiency of conversion into the second and third harmonics of neodymium at a level of 80–90%. This opens up extremely interesting possibilities for attaining record-setting high pressures in shock waves generated by lasers. In this connection we note Ref. 83, in which shock waves with a pressure of 10–12 Mbar were obtained for the first time by using the radiation of the third harmonic of a neodymium laser.

f) Radial expansion of the energy-release region at high intensities

It has been established experimentally[42] that the dimension of the high-temperature region of the target determined with an x-ray camera exceeds approximately fivefold the dimension of the focal spot of the laser beam *in vacuo*. At the same time, the amplitude of the shock wave recorded in these experiments is an order of magnitude smaller than the theoretical predictions of (3.4) (see Fig. 7). A special series of experiments[43] found during the irradiation of a laser target a considerable emission from the wire grounding the target, which they attributed in Ref. 43 to Joule heating by the high-power reverse currents bringing about the electric neutrality of the target. In line with the measurements of Ref. 43, this heating wave has the characteristic velocity of $\sim 10^8$ cm/s. The following interpretation of the experiments of Refs. 42 and 43 has been proposed in Refs. 41, 45, and 46. The laser radiation incident on the plasma is absorbed near the critical surface, and generates nonthermal electrons. On leaving the plasma, the latter break down the electric neutrality in the region of light absorption. Consequently compensating currents of cold electrons arise and arrive from the unirradiated parts of the target. At characteristic times of $\sim 10^{-10}$ s, such currents must be surface currents (the thickness of the skin layer is of the order of 10^{-4} cm), while their density must reach 10^{10}–10^{12} A/cm^2, which can cause the evaporation and glow of the targets observed in Refs. 28 and 43. The concept of compensating currents has been discussed also in Refs. 27, 41, and 46.

The employment in later studies[147,157,158,165] of a refined experimental technique has enabled fuller study of the processes of radial expansion of the heated region on the surface

of laser targets. It has been established[158] by high-speed photography that the velocity of propagation of the "heating wave" in the radial direction amounts to 2×10^8–2×10^9 cm/s at laser intensities in the range 10^{15}–$2\cdot10^{16}$ W/cm^2. A system of x-ray filters was used to isolate the K_α line of the target material and to measure its intensity quantitatively. Since the only way of exciting the K_α line under the conditions of the experiments of Ref. 158 is the ionization of the K-shell of the target material by fast electrons, the conclusion was drawn in this study that the heating of the target outside the focal spot results from collisions with the target of nonthermal electrons generated in the absorption zone. Quantitative measurements of the K_α radiation with spatial resolution showed that the fast electrons release up to 30% of the absorbed laser energy at a distance of several millimeters from the focal spot.

A characteristic feature of the radial dissipation of energy that was clearly observed in the experiments of Ref. 158 is that the time-integral energy release reaches a maximum near the edge of the heated region, rather than at the edges of the focal spot (Fig. 18).[4)] This renders the possibility of any appreciable contribution of the compensating currents to the heating unlikely. At the same time the question arises of the mechanism of generation of the fast electrons. If they involve resonance absorption (which plays a substantial role under the conditions of the experiments being discussed), then it becomes necessary for strong quasistatioary fields to exist in the plasma that might "focus" the electrons, or we must assume that there is a considerable deformation of the critical surface. It is simpler to explain the observed pattern if we assume that the nonthermal electrons result from Langmuir collapse.

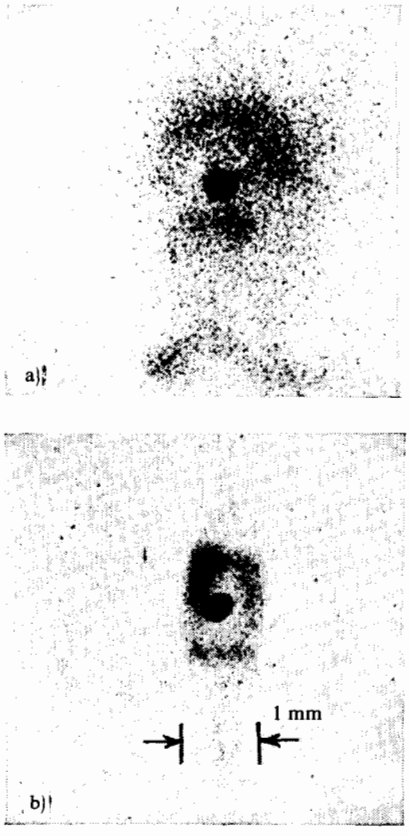

FIG. 18. Image of a target obtained with an x-ray camera obscura. Target material: Cu. Iodine-laser pulse of durations 300 ps and intensity $6\cdot10^{15}$ W/cm^2. a) Target of large area; b) target of area 1 mm^2. The thickness of the target is greater than the mean free path of the fast electrons.

[4)]The authors thank Dr. K. Aĭdman for providing the original of Fig. 18.

We note that interesting effects of energy transport by fast electrons have also been observed in experiments with CO_2 lasers, where they were manifested at lower intensities (see Refs. 159, 160, and 165).

g) The "internal" structure of laser shock waves

In order than one may use the relationships (1.1) for diagnostic purposes, the characteristic dimension of the densification jump δ must be much smaller than the thickness of the layer of shock-compressed plasma $l = x/\sigma$. Here $\sigma = \rho/\rho_0$ is the degree of compression of the material in the shock wave that has passed through the distance x in the target.

The internal structure of the shock jump is determined by the transport processes in the shock-compressed plasma. The viscous densification jump in solids has a characteristic dimension of several interatomic distances, while the inhomogeneities of the front estimated from optical measurements[2] in any case do not exceed a wavelength of light. The thermal radiation leaving the front at $p\sim80$–100 Mbar has characteristic frequencies ν_m (the frequencies corresponding to the Planck maximum; see Table II) less than the plasma frequency of aluminum ahead of the breakdown front $\omega_p = 5\cdot10^{15}$ s^{-1}. Thus this radiation is localized in a thin layer ahead of the front of the shock wave. Resonance screening is absent starting at shock pressures ~10 Mbar, and we can take the characteristic dimension of the heated zone to be the mean free path of the radiation, which is determined by the free-free transitions l_{ff}. We see from Table II that even by itself this absorption mechanism brings about effective screening at pressures up to hundreds of megabars, while taking photoionization into account shifts this boundary up to pressures of thousands of megabars.

The relaxation structure of the shock wave is determined by energy transfer from ions to electrons:

$$l_{ei} = D\tau_{ei}\sigma^{-1}.$$

Under typical experimental conditions this exchange is carried out extremely rapidly (see Table II).

For estimates of electron transport in the wave front let us replace the front with an emitter that emits electrons with an energy $\varepsilon_e \sim T_h$. We shall estimate the mean free path of these electrons in cold aluminum by adopting for the cross-sections of electron-ion scattering[47,48]:

$$\sigma = \frac{\pi e}{2\varepsilon^2}\ln\left[1+\left(\frac{r_e\varepsilon}{e^2}\right)^2\right].$$

This yields values $l_{ei}\sim10\,\mu$m for waves of extreme intensity (Table II).

h) Results of numerical simulation

Owing to the great complexity of the physical processes in a high-pressure laser plasma, at present one can describe

TABLE II. Transport processes in a shock wave-front in aluminum.

p, Mbar	T, eV	V, cm^3/g	ν_m, s^{-1}	λ_m, cm	$h\nu_m$, eV
1	0.6	0.203	$3.9\cdot10^{14}$	$7.7\cdot10^{-5}$	1.7
10	8	0.118	$5.2\cdot10^{15}$	$5.7\cdot10^{-6}$	22.4
100	50	0.083	$3.3\cdot10^{16}$	$9\cdot10^{-7}$	140
1000	400	0.075	$2.6\cdot10^{17}$	$1.2\cdot10^{-7}$	$1.1\cdot10^{3}$

l_r, μm	τ_{ei}, s	$l_{ei}=u\tau_{ei}$, cm	D, km/s	σ	l_e, cm
$2.7\cdot10^{-7}$	$4\cdot10^{-16}$	$2\cdot10^{-10}$	9.1	1.8	$2\cdot10^{-8}$
$7\cdot10^{-5}$	$1.15\cdot10^{-14}$	$8.8\cdot10^{-9}$	23.3	3.1	$3.6\cdot10^{-8}$
0.16	$1.24\cdot10^{-13}$	$1.9\cdot10^{-7}$	69	4.5	$3.7\cdot10^{-7}$
80	$2.5\cdot10^{-12}$	10^{-5}	215	5	$1.2\cdot10^{-5}$

them quantitatively only by numerical methods. Here we shall examine the results of calculations by the program LASNEX[34] of the dynamics of motion and heating of an aluminum plasma under conditions characteristic of the experiments on laser generation of shock waves.[27,28] The thermodynamic properties of the plasma were described by a quasiclassical model supplemented by taking ionization equilibrium into account. The calculations of laser absorption took into account decelerating processes and resonance absorption (efficiency $\sim 30\%$), which give rise to nonthermal electrons with a Maxwell spectrum and the temperature T_h of (4.4). The electron heat flux in the plasma was restricted by ion-sonic turbulence up to the drift velocities, which are proportional to the velocity of ionic sound.[49] We note that precisely the electron transfer and the nonthermal electrons are least reliably described by this method. Hence appropriate experiments must be carried out—pending performance of the thermodynamic measurements.

The main series of calculations[39] was performed for a laser intensity of $\sim 2\cdot10^{14}$ W/cm^2 and an aluminum target with a characteristic thickness of 25 μm. The laser pulse with a half-width $\tau = 300$ ps had a triangular shape with rise and fall times of 300 ps. Longer pulses had the form of a trapezoid with rise and fall times of 300 ps and with a region of constant intensity.

The results of the calculations[39] show (Fig. 19) that the nonthermal electrons in the chosen example raise the initial temperature of the target up to ~ 0.5 eV, which amounts to 10% of the temperature of shock compression. The sharp fall in the parameters behind the front of the shock wave (Fig. 19) can arise both from the triangular shape of the laser pulse and from the strong rear unloading. The analysis presented in Ref. 39 shows (Fig. 20) that, out of the 35 J of the energy absorbed by the plasma, 21 J and 14 J are imparted to the thermal and the nonthermal electrons. Here the nonthermal electrons then transfer 11 J to thermal electrons, 1.5 J to ions, 0.8 J goes directly into energy of motion, and 0.06 J into radiation. Out of the energy of the thermal electrons, 21 J is converted into the kinetic energy of the plasma flux, and 5.5 J is lost by radiation upon recombination. Consequently the thermal energy of the ions amounts to 0.5 J, that of the electrons is 6.4 J, while 22.8 J is converted into the kinetic energy of the flux. Here a large part of this energy is imparted to the ions of the expanding corona. The hydrodynamic efficiency of the process (ratio of the kinetic energy of the shock-compressed part of the target to the laser energy) amounts to $\sim 1\%$.

The relationship of the parameters of the plasma to the intensity and duration of the laser pulse is shown in Figs. 21 and 22. We see that, when $I \approx 5\cdot10^{14}$ W/cm^2, the heating on a baseline $d \approx 25$ μm is too large, and it does not permit one to determine the shock adiabat from the relationship (2.1). However, in this region other interesting physical experiments can be performed that employ fast electron heating.[98] The decrease in the maximum p and T with decreasing duration of the pulse in Fig. 22 arises from the rear unloading waves. Here also the relative overheating of the target by nonthermal electrons is diminished. However, this regime corresponds to a considerable damping of the shock wave that hinders application of Eqs. (2.1). Figure 22 illustrates the difficulty of experiments with homogeneous targets at intensities $I \gtrsim 2\cdot10^{14}$ W/cm^2 ($p > 15$ Mbar) arising from the

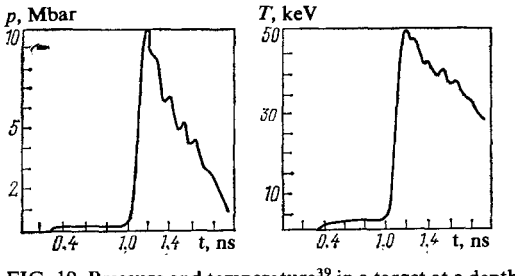

FIG. 19. Pressure and temperature[39] in a target at a depth of 25 μm for a neodymium-laser intensity $I = 2\cdot10^{14}$ W/cm^2 and pulse duration $\tau = 300$ ps.

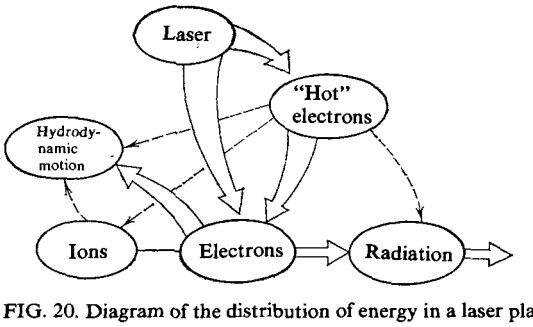

FIG. 20. Diagram of the distribution of energy in a laser plasma.[39]

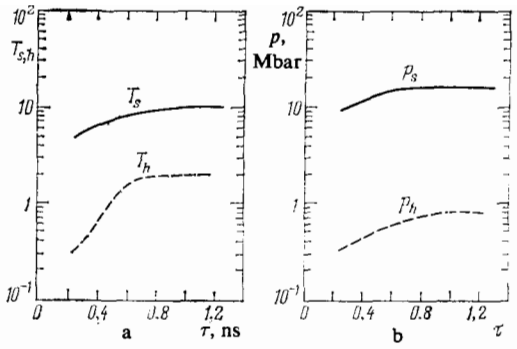

FIG. 21. a) Dependence on the duration τ of the laser pulse of the temperature T_s of shock compression and of the temperature T_h of heating by nonthermal electrons in an aluminum target at a depth of 25 μm for $I = 2\cdot10^{14}$ W/cm^2 [39]; b) dependence on the duration of the laser pulse of the pressure p_s of shock compression and of the pressure caused by nonthermal electrons in an aluminum target at a depth of 25 μm.[39]

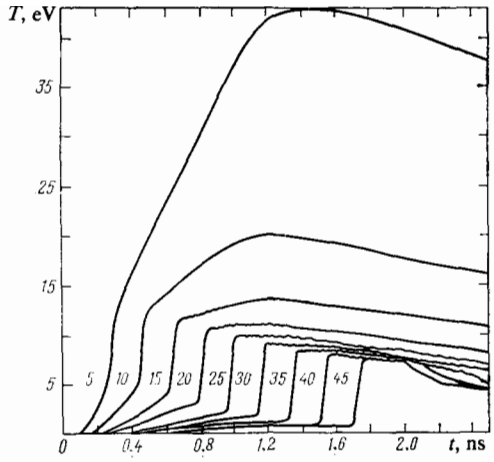

FIG. 23. Time profile of the temperature at different cross-sections (distance from the irradiated surface in μm) of an aluminum target for $I = 2\cdot10^{14}$ W/cm^2 and $\tau = 900$ ps.

unfavorable relationship between the initial temperature T_0 of the target and the temperature of shock compression T_ξ. Thus, for $I > 10^{15}$ W/cm^2, we find $T_0 \sim 0.5T_\xi$ owing to the preliminary heating, and the shock wave in this case is a relatively weak "perturbation". This leads us into a region of interesting hydrodynamic experiments, but a direct determination of the shock adiabats will be difficult here. the role of the electron heating is pictorially illustrated also by Fig. 23, which shows the temperatures of the plasma at different cross-sections of a target irradiated with a pulse with $I = 2\cdot10^{14}$ W/cm^2, $\tau = 900$ ps.

To determine the relative compressibility of metals,[14] one must determine the wave velocities in the transition of the wave from one element to another. The maximum pressure at the front of a shock wave in a target consisting of layers of aluminum and tungsten is shown in Fig. 24, which shows that a sharp growth in the shock pressure occurs at the instant of reflection of the shock wave from the tungsten, since the dynamic rigidity ($\rho_0 c_s$) of tungsten exceeds that of aluminum. The calculations showed that the effects of preliminary heating of the target (Fig. 25) at the instant $t = 300$ ps, starting with $x = x_c \sim 20$ μm, are not very substantial. We note that the effects of generation of spontaneous magnetic fields[50] not taken into account in the one-dimensional calculations can increase the energy of the nonthermal electrons, and correspondingly increase x_c. Curiously, in the hydrodynamic calculations[39] by the single-group approximation, the radiation heating was estimated, whose effect (in agreement with the remarks in Sec. 4) proved to be negligibly small. The electron temperature of the plasma measured in experiments with electron-optical converters on different baselines of measurement has been calculated in Ref. 39 (see Fig. 23). We see an appreciable decrease in the role of the preliminary heating with increasing thickness of the specimen being studied.

In closing this section, we note again that the fundamental restriction in the laser experiments analyzed here is the preheating of the target by the nonthermal electrons. This effect leads to a need for applying relatively long pulses and to an unfavorable dependence of the laser energy on the chosen plasma pressure in (4.6). Hence it seems that upward advance along the pressure scale in laser experiments can follow two lines: by increasing the frequency of the laser radiation and by using layers of heavy elements to absorb the nonthermal electrons. Progress along the former of these lines depends on the possible creation of high-power short-wavelength lasers and efficient frequency-converters. In addition to the direct screening of the flux of nonthermal elec-

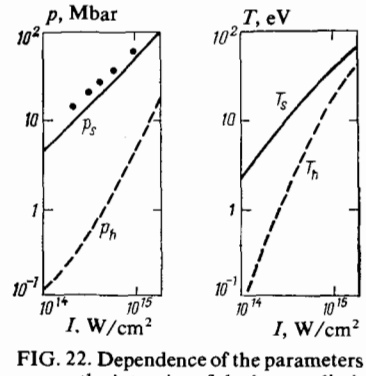

FIG. 22. Dependence of the parameters of an aluminum plasma at $d = 25$ μm on the intensity of the laser radiation for a fixed duration of the laser pulse $\tau = 300$ ps. Dots—data for longer pulses.[39]

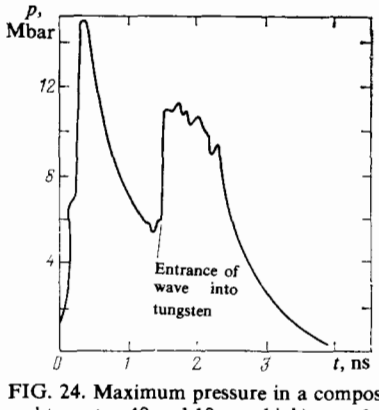

FIG. 24. Maximum pressure in a composite target (layers of aluminum and tungsten 40 and 10 μm thick) upon laser irradiation.[14] Energy: 50 J, $\tau = 250$ ps.

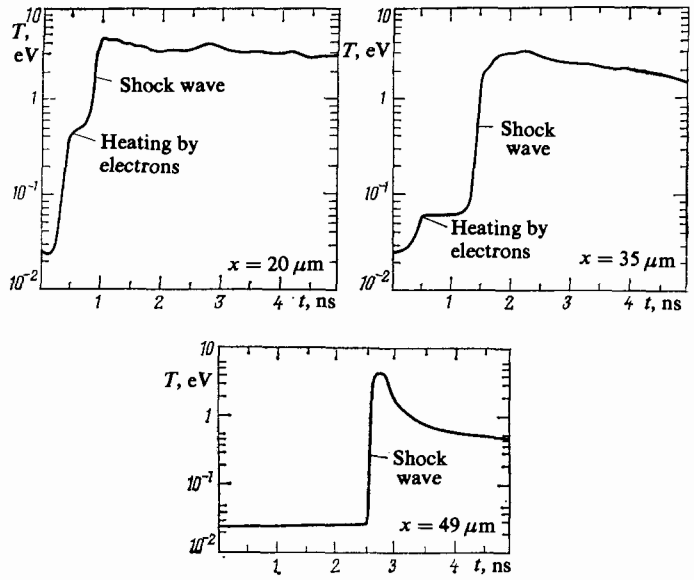

FIG. 25. Temperature profiles at different cross-sections of a composite target for radiation parameters of 50 J/250 ps.[14]

trons, the use of layers of multielectron heavy elements enables one to improve the hydrodynamics of the entire flow, since these layers, being heated by the shock wave and by the nonthermal electrons and playing the role of a heavy piston, will efficiently maintain the shock wave in the material being studied. Thus, according to Ref. 39, introduction of a tungsten layer 3-μm thick extends the damping time of the shock wave to hundreds of picoseconds, cuts in half the size of the heating zone, and in agreement with the analysis in Sec. 4, decreases the needed laser energy by almost an order of magnitude.

5. DIAGNOSTICS AND EXPERIMENTS

a) General requirements on targets and diagnostic means

In line with the general rationale of dynamic experiments,[1] to study the equation of state one must independently measure any two of the five parameters characterizing the propagation of the plane steady-state shock discontinuity: D, u, p, V, and E, and then calculate the rest of the parameters from the general conservation laws (2.1). This enables one to find the equation of state of the studied material in the caloric form $E = E(p,V)$. In dynamic experiments it is easiest and most accurate to record the phase velocity of motion of the shock wave D by baseline electric-contact and optical methods.[1,3,5] With the five baselines of measurement estimated in Sec. 4 of $\sim$20–50 μm and velocities of movement of the discontinuity of 20–50 km/s, the characteristic time of the experiment proves to be of the order of 1 ns. This rules out the use in laser experiments of electrical contacts, whose time of operation can hardly be shortened to values less than hundreds of picoseconds.[89] Hence optical methods are preferable here for physical detection.

In opaque materials the shock wave can be fixed at the instant of emergence at the free surface of stepped targets.[14,27,28,53,83] Here it becomes visible whenever it approaches to a distance of several mean free paths of light l_r from the free surface. For the optical range in metals we have $l_r \sim 10^{-5}$ cm.[14] At a velocity of motion $D \sim 20$ km/s, this leads to a rise in the light signal int he time $\tau \sim l_r/D \sim 5$ ps,[14] which determines the necessary time resolution of the electro-optical converters used in these experiments. The emissive properties of the surfaces of stepped laser targets heated by the shock wave or by the nonthermal electrons up to temperatures of several electron volts have been treated in Ref. 89, where the model of electron transport in a dense plasma was used for this purpose.

With characteristic baselines for measuring the vleocities of motion of shock waves of $\sim$20 μm, the necessary accuracy of preparing and measuring the baselines of the targets proves to be $\sim$0.1 μm. This makes possible an accuracy of measurement of $\sim$2–3%, which suffices for an experimental test of theoretical models of equations of state. According to the criteria of Sec. 4, with increasing duration of the laser pulse the baseline of measurement also increases, and this increases the accuracy of measurement. If the transport and relaxation processes have larger characteristic times than estimated in Sec. 4, one can measure the corresponding spatial structures experimentally from the increase in the light signal with time. The needed spatial resolution of the high-speed camera is determined by the transverse dimensions of the target, and must be no poorer than 10 μm.

Thus experiments with laser shock waves require a refined technology of preparing and preliminary monitoring of the characteristics of plane homogeneous microtargets. To prepare such targets, one applies the methods of ion bombardment and deposition of metals from the gas phase, which allows one to obtain steps with a deviation from planarity of the surface $\lesssim$0.1 μm.[83] To measure the dimensions of targets, methods of optical, electron, and interference microscopy are utilized. In the latter case the accuracy of measurement of the height of a 5-μm step amounts to $\sim$1%.[83] For local (up to 50 μm) measurement of the density of the target material, the use is discussed in Ref. 83 of the method of low-energy proton scattering, which yields an accuracy of

measurement of $\sim 1\%$.

In transparent materials one can illuminate[35,42] the target from the side with an external light source. The shock wave absorbs or changes the direction of this light flux, while the slope of its trajectory of motion in the x–t diagram determines D. Moreover, one can take time-lapse pictures of the interferometric pattern of motion of the material of the target.[91] Evidently the accuracy of these two methods is less than that of the "step" method that was realized in Refs. 27–29, 83, and 90. We note that one can use reflection of the laser radiation from the surfaces of stepped targets to fix the instant of exit of the shock wave at given baselines, and also one can utilize fiber optics.[164]

Measurement of the second dynamic parameter involves substantially greater difficulties. In dynamic experiments using the explosive technique[1] and light-gas propellant apparatus,[88] the "reflection" method[1,5] has been most widespread for determining the mass velocity u of the shock-compressed material. This is based on applying the general gasdynamic laws that arise in the decay of an arbitrary discontinuity. The concrete measurements are reduced to determining the phase velocity of motion of shock waves in the studied material and in a "standard" (a material with a known shock adiabat). Owing to the condition of continuity of the pressure and velocity at the contact boundary, this enables one to find the mass velocity of motion of the studied material. The independent determination of the shock adiabat of the "standard" is performed by the "braking" method,[1,5] in which one determines the velocity of the shock wave in the standard the velocity of flight $w = 2u$ of a projectile made of the material of the "standard". The "reflection" method, which is fundamental in high-pressure dynamic physics, has permitted determining the shock compressibility of a large number of chemical elements and compounds. The handbooks of Refs. 36, 92 give the characteristics of more than 300 materials studied thus far at pressures up to ~ 5 Mbar. Shock pressures of tens of megabars have been obtained by using the technique of strong underground explosions[10,11,24,93] and detonation of nuclear charges.[25] For these pressures the problem of standards presents difficulties since the application of the "braking" method is difficult here. In this case one can measure only relative compressibilities of materials using the adiabat of the standard extrapolated beyond the limits of the region of direct measurements. Here one uses as standards elements of high atomic number, for which the quantum statistical calculations are most reliable. An essential point is that, in constructing the standard shock adiabats in this case, one must resort to long-range extrapolations (from 5 to 300 Mbar),[8,24,25] while the uncertainty arising here (reaching 50% in pressure[8]) is transferred to the subsequent measurements.

In Ref. 25 a direct measurement was made of the velocity u at pressures $p \sim 20$ Mbar from the Doppler shift of the resonance lines of neutron absorption of molybdenum, which was chosen as the standard. The results obtained agree reasonably well with the measurements at lower pressures.[94] A measurement[10] of the mass velocity of aluminum at a pressure ~ 10 Mbar by the baseline method from the motion of a γ-reference point showed substantial discrepancies of the measurements from the predictions of the quantum statistical theory. This called into question both the extrapolation calculations themselves and the interpretation of the relative measurements based on them.[8] In laser experiments the reflection method has been used in Ref. 53 for the aluminum-gold pair and in Ref. 90 for the aluminum-copper pair.

Thus, despite the known uncertainty in the parameters of standards at $p > 5$ Mbar, the reflection method apparently enables one to measure most simply the group velocity of motion of the material in laser experiments. Here molybdenum will probably be used as the standard, for which absolute measurements have been made up to $p \sim 20$ Mbar, or aluminum, for which detailed dynamic measurements have been made,[36,92–94] and quantum-mechanical calculations have been made of the equation of state.[95]

The method of determining u proposed in Ref. 14 is based on using a high-speed x-ray detector to measure the displacement of the contrast boundary of the heavy and light material with lateral x-ray illumination of a layered target.[97] According to the estimates,[14] this method can yield an accuracy of measuring u of the order of 6–8%.

The next generations of laser experiments will determine a more complete set of physical parameters besides the kinematic characteristics. At the considerable compressions of matter in shock waves of extreme intensity, the determination of the wave and mass velocities of motion is not optimal from the standpoint of determining the equation of state. In this case it would be desirable to measure directly the degree of compression of the plasma in the shock wave, along with D, either by x-ray absorption, as has been done in Refs. 3, 54 for a nonideal plasma, or from the Stark broadening of the spectral lines in the x-ray region of the spectrum.[55] Temperature measurements (pyrometric or Doppler-spectral) are very useful, since one can expect considerable nonmonotonicity, specifically in the temperature-dependence, owing to manifestation of the shell structure at high pressures.

Experiments with plane steady-state shock waves amount to the simplest and most easily interpreted type of experiments to study the properties of a material at high temperatures and pressures. However, the use of high-power lasers also opens up other interesting possibilities in the experimental physics of high energy densities. Irradiation of thin ($1 \sim 10$ μm) metallic targets with laser radiation with $I\lambda_0^2 > 10^6$ W leads to heating of the opposite side of the target by nonthermal electrons.[98,99,41,159] By comparing the measured temperature with the data of calculations,[65,102] one can correct the theoretical models pertaining to this phenomenon, which is as yet poorly studied. At smaller values of $I\lambda_0^2$, one can study by this method the features of electron heat conduction in a laser plasma.[100–102] We note that nonthermal electrons are an efficient source of fast bulk heating of a condensed material up to temperatures of several electron-volts. The decay of such high-temperature states has been employed[103] to generate strong shock waves.

As we know, in a single shock compression the density

of the compressed material cannot exceed a certain bound. Therefore, in the simplest experiments with a single stationary shock wave, the extremely interesting region of the phase diagram corresponding to supercompressed matter proves to be unattainable. A number of approaches has been proposed for advancing into this region, a common feature of which is the smallness of the increase in entropy in compression. In experiments with high-power lasers, one can use a sequence of several pulses optimally chosen in amplitude and frequency, instead of a single pulse, or else a single continuous pulse of special form with increasing intensity.[161,56,57] Instead of programming the laser pulse, one can use a layered or shell target with a specially chosen initial density profile. Several other possibilities have been discussed in Ref. 162. We note that the problem of measuring the parameters of the compressed material becomes very complicated in all experiments with quasi-isentropic compression. Experiments of similar design oriented toward the problem of laser thermonuclear fusion have employed x-ray photography, spectroscopy of multiply-charged ions, detection of the products of thermonuclear reaction and indirect methods based on measuring the parameters of the corona. The method of measuring shock waves at a considerable distance from the focusing site of the laser radiation shows definite promise. Application of the theory of a point explosion[59] makes it possible to estimate the effective energy of the explosion.[38]

Laser methods can be useful not only in studying strongly compressed matter with a density exceeding that of the solid. By using the expansion of a material heated by a laser shock wave or by nonthermal electrons,[103] one can obtain a broad spectrum of states in the isentropic unloading wave, including the region of the Boltzmann strongly nonideal plasma, the neighborhood of the high-temperature boiling curve, and the region of the "metal-dielectric" transition.[3,60]

Even a short list of the possible experiments at very high local energy concentrations attainable with modern lasers shows that this technique has vast advantages over other methods of obtaining high pressures, and it allows one to obtain new physical information on extreme states of matter. Naturally, the measurements here lie at the boundary of modern high-speed recording technique, while the interpretation of the experiments requires introduction of new physical models and complicated numerical calculations.

In closing, let us examine the as yet few experiments on laser generation of shock waves in solids and discuss the effects associated with this method of generation.

b) Experiments with laser shock waves

The first experiments on excitation of shock waves in solid hydrogen and in Plexiglas were performed with a low-power neodymium laser[35] with an energy of $E \approx 12$ J and a pulse duration $\tau = 5$ ns. Owing to the small dimension (~ 40 μm) of the focal spot, the shock waves with a maximum pressure ~ 2 Mbar rapidly became spherical and decayed. A shock pressure in polyethylene of ~ 1.7 Mbar has been obtained[110] at a radiation intensity $I = 3.5 \cdot 10^{14}$ W/cm^2, while the amplitude pressure for $I = 2 \cdot 10^{14}$ W/cm^2 amounted[114] to ~ 2 and 4 Mbar respectively in hydrogen and Plexiglas. Measurement of the ions of the plasma corona and the recoil momentum of the target (integral methods) made possible an estimate[82] of the pressure in an aluminum target at $I \approx 10^{14}$ W/cm^2. The value of the exponent in Eq. (3.4) found from these measurements was $\alpha = 0.8$. A more powerful laser system based on neodymium glass with an energy $E \sim 20$–40 J, $\tau = 0.3$ ns, and $I = 3 \cdot 10^{14}$ W/cm^2 was used[28,109] to obtain plane shock waves. Velocities of the front of a shock explosion of 13 km/s (corresponding to a pressure ~ 2 Mbar) were determined from the time of passage of the shock wave through a stepped aluminum specimen. Also the velocity of dispersal of the plasma corona was measured. The measurement of the time rise in the radiation intensity upon exit of the shock wave at a free surface ($\Delta t \leqslant 50$ ps) yielded an estimate of the thickness of the shock discontinuity of $\lesssim 0.7$ μm. The authors note the poor reproducibility of the energy of the laser radiation and the appreciable asymmetry of the focal spot.[28,109] The shock pressures were increased[27] by an order of magnitude (Fig. 26) by using the "Janus" laser[112] with larger parameter values: $E \approx 100$ J, $\tau = 300$ ps. Radiation intensities $I \sim 8 \cdot 10^{13}$–$3 \cdot 10^{14}$ W/cm^2 were obtained in a focal spot of diameter 300–700 μm. In Ref. 27 a target of small diameter was used. In the opinion of the authors it decreased the effect of surface currents,[43,44] and agreement between theory[96] and experiment was obtained (Fig. 7 of Ref. 27). Subsequent experiments in this apparatus made it possible[83] to find the value of the exponent in Eq. (3.4): $\alpha = 0.65$ in the range of radiation intensities $5 \cdot 10^{13}$–$5 \cdot 10^{14}$ W/cm^2.

Record-setting plasma pressures $p \approx 35$ Mbar were obtained[83] under the action of the radiation of a neodymium laser with $\lambda_0 = 1.05$ μm upon irradiating a target consisting of a layer of aluminum 22-μm thick and a layer of gold 32-μm thick with ten overlapping beams of the laser installation "Shiva".[113] The maximum intensity was $2.9 \cdot 10^{15}$ W/cm^2 with a pulse duration of 625 ps.[5)] The measured velocity of the shock wave in gold amounted to 17.3 ± 0.3 km/s. This agreed with a two-dimensional hydrodynamic calculation[96] in which the fraction of the energy absorbed in the plasma

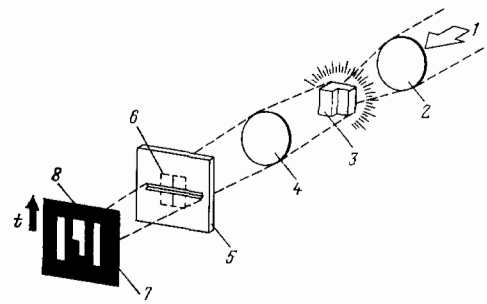

FIG. 26. Diagram of experiments on laser generation of shock waves.[27,28,29] 1—laser radiation; 2—focusing system; 3—stepped target; 4—optics of electro-optic converter; 5—slit of electro-optic converter; 6—image of target; 7—photographic film; 8—image being recorded.

[5)] A report had been made earlier[29] of a pressure fo 40 ± 4 Mbar obtained with a somewhat larger target (22 μm of aluminum, 50 μm of gold) using the same laser equipment ($E = 3.8$ kJ, $I = 2.4 \times 10^{15}$ W/cm^2).

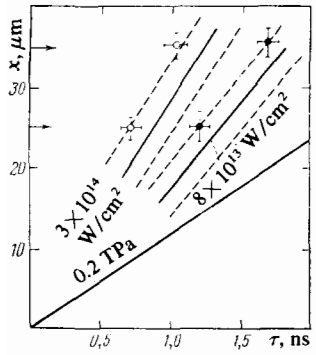

FIG. 27. Comparison[27] of the measured times of arrival of the shock wave at the free surfaces of stepped aluminum targets (arrows) with those calculated by a hydrodynamic program.[96] The regions limited by the dotted lines correspond to a 10% change in the area of the focal spot and the fraction of absorbed energy. The lower line is the trajectory of a steady-state shock wave with a pressure of 0.2 TPa.

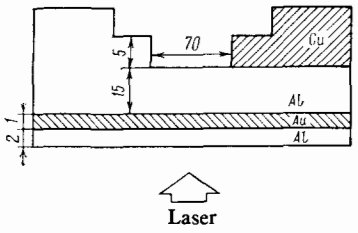

FIG. 28. Diagram of a layered laser target[90] in the "reflection" method (dimensions in μm).

was equal to 30% and the convergence of the laser beam was taken into account.[87] The measurements of the x-ray emission spectrum in this experiment made possible an estimate of the heating of the rear of the target by nonthermal electrons. It proved to be less than 500 C, while the temperature of the shock-compressed plasma was of the order of 5 eV.

A variant of the "reflection" method was realized in the experiments of Ref. 53 with a layered target, in which passage of shock waves of amplitude $p \sim 3$ Mbar from aluminum to gold ($p \sim 6$ Mbar) was realized under low-damping conditions. Just as in Ref. 28, the laser radiation ($E \sim 20$–30 J, $\tau = 300$ ps) was nonuniformly distributed over the focal spot, the shape of which varied from circular (diameter 100 μm) to elliptical (with axes 200 and 500 μm). In the opinion of the authors,[53] the latter circumstance was the main cause of error in these experiments. Within the limits of accuracy of the measurements ($\delta D = 15\%$, $\delta p = 30\%$), the data[53] agree with the theoretical models of the equation of state introduced for comparison, although this accuracy proved insufficient for choosing the best model. In the studied range of parameters, the deviation among the models did not exceed 10%.

Systematic studies of the shock compressibility of aluminum and copper by the comparative method were performed in the "Janus" laser system[90] in the intensity range $I \sim 5\times10^{13}$–4×10^{14} W/cm^2, $E \sim 30$ J, $\tau = 300$ ps). A thin layer of gold in the target (Fig. 28) was employed to absorb the nonthermal electrons and to increase the duration of the shock wave (however, while somewhat reducing the maximum pressure). The preliminary results that were obtained (Fig. 29) pertain to the pressure range 2–6 Mbar in aluminum and 4–8 Mbar in copper. These agree well with the results of dynamic experiments performed with powerful explosives and light-gas propellant devices.[94,123] Subsequently the authors of Ref. 90 have proposed reducing the error of measurements from ~10% to 2% and elevating the pressure in aluminum to 12 Mbar in the "Janus" installation and to 30–40 Mbar in the "Novetta-Shiva" installation.

In addition to the reflection method in laser experiments, a method has been developed[97] of measuring the velocity of motion of the plasma by the method of pulsed x-radiography (Fig. 30). An aluminum target (*2*) 17-μm thick is irradiated with a laser beam (*1*) of the "Shiva" installation with an intensity $I = 6\cdot10^{14}$ W/cm^2 ($E = 110$ J, $\tau = 600$ ps). Here one of the beams of this instrument (*4*) was incident on a tantalum target (*5*), which yielded x-rays with the characteristic energy 1.9 keV. The pattern of motion in the field of the x-rays was determined with a high-speed x-ray camera (x-ray "microscope"[97]) with time and space resolutions of 15 ps and 4.5 μm. This made it possible to find that the velocity of motion of the plasma is $8\cdot10^6$ cm/s. A strong lateral spread of the plasma that screened the x-ray illumination was noted.[97] Apparently this method will be employed in the future for measuring the mass velocity of motion of plasma by determining the contrast boundary for x-rays betwen the light and heavy material.[14]

The experiments performed[83] on generating shock waves with short-wavelength laser radiation are of special interest, since enhanced amplitude pressures of the shock-compressed plasma are predicted for these regimes, owing to the increased fraction of the absorbed laser energy and the suppression of the nonthermal electrons (Sec. 3). Laser radiation with $\lambda_0 = 0.35$ μm and intensity $(1$–$2)\cdot10^{14}$ W/cm^2 ($\tau = 700$ ps) was used to irradiate an aluminum target 25-μm thick, in which a shock wave arose with a pressure 10–12 Mbar. Here the energy absorbed by the plasma amounted to ~95% of the incident flux. In the same experimental arrangement, irradiation with long-wavelength radiation at $\lambda_0 = 1/06$ μm with $I = 3\cdot10^{14}$ W/cm^2 (the absorbed energy was 1.2×10^{14} W/cm^2) yielded a pressure ~6 Mbar.

In Ref. 103 the results are given of determining the motion of shock waves, of the free surfaces, and of the plasma corona upon irradiating aluminum targets 50–200 μm thick

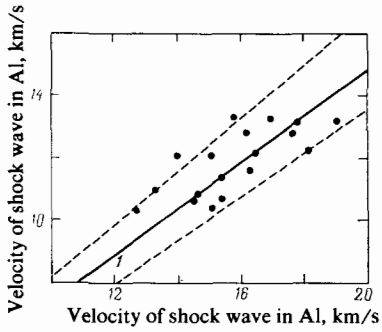

FIG. 29. Results of experiments by the "reflection" method.[83,90] 1—extrapolation of the experimental data[123] (dotted lines p—10% error); dots—results of Ref. 90.

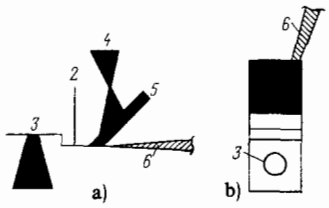

FIG. 30. Diagram of an experiment with x-ray illumination of the target.[97] 1—laser beam generating a shock wave in the target; 2—Mylar screen; 3—target being studied; 4—laser beam for x-ray illumination; 5—tantalum target generating x-rays; 6—support of experimental setup; a) side view; b) top view.

with the radiation of the GEMINI CO_2 laser with $E = 150$ J, $\tau = 1.1$ ns, diameter $\sim 600\ \mu$m at an intensity $I = 4.5 \cdot 10^{13}$ W/cm^2. The shadow pattern obtained with lateral illumination with an argon laser shows a sharp inhomogeneity of flow in the corona and steepening of the density profile caused by light pressure and by the recoil momentum of the fast electrons.[115–117] The measured velocity of dispersal of the corona amounts to $2.6 \cdot 10^7$ cm/s. The experiments measured the velocity of dispersal of the free surface of the target, which yields an estimate of the pressure in the shock wave $p \approx 5$ Mbar. This somewhat exceeds the value obtained in hydrodynamic calculations.[96]

c) Experiments on heating with fast electrons. Anomalous energy transport

An intense flux of nonthermal electrons with $T_h \sim 15$ keV arising in the resonance-absorption zone was used[98] for exploding a thin layer of aluminum with the aim of generating shock waves with $D = 2.5 \times 10^6$ cm/s in a target of thickness $d \sim 10$–$40\ \mu$m. A CO_2 laser system[114] with an energy $E = 50$ J, $\tau = 800$ ps, and intensity $I = 3 \cdot 10^{14}$ W/cm^2 made it possible to obtain values of the parameter $I\lambda_0^2$ two orders of magnitude higher than in typical experiments with neodymium lasers.[27,28,53,111] Under these conditions, from 30 to 50% of the absorbed laser energy went into generating fast electrons,[118] which on being decelerated isochorically heated a thin ($\sim 3\ \mu$m) layer of aluminum. Upon expansion of this layer a shock wave was formed with a pressure $p = 13$ Mbar. In these experiments the overall hydrodynamic efficiency amounted to 10–15%. We note that, according to the estimates of Ref. 91, appreciable heating of the medium occurred ahead of the shock wave that elevated the pressure to about 3 Mbar.

The results of experiments to study the heating of a target by nonthermal electrons[41] showed that, on a baseline of 25 μm at $I \sim 10^{14}$–10^{15} W/cm^2 ($\lambda_0 = 1.06\ \mu$m), the temperature of this heating was smaller by more than an order of magnitude than the estimated values (~ 12 eV). Experiments performed with smaller intensities and target thicknesses[101] made possible a study of the heat conductivity of a laser plasma with establishment of a considerable (10–15-fold) restriction of the heat flux as compared with the classical value. This restriction is associated in the paper with thermoelectrically generated magnetic fields, which had an induction $B \sim 10^6$ G.[102]

A number of papers[41,43,98,103,104,147,157–160] have studied experimentally the anomalous surface energy transport that effectively enlarges the focal spot and reduces the laser intensity. This effect involves the generation of nonthermal electrons and is manifested most strongly in experiments with CO_2 lasers. The interaction of the radiation of a CO_2 laser of intensity $2 \cdot 10^{14}$ W/cm^2 with aluminum targets of varying diameters and of thicknesses from 12.5 to 150 μm was studied in Ref. 104. In addition to measuring the anomalous transport, these experiments observed accelerated ions with a characteristic energy 0.6 MeV.

d) Experiments on ablative acceleration

Great potentialities for generating strong shock waves are offered by ablative acceleration of thin foils and films up to velocities of 10^6–10^7 cm/s when acted on by laser radiation. When these foils collide with targets, shock waves are generated with a square-wave pressure profile. The effects of preheating of the target by fast electrons and x-rays become far less significant. Moreover, the method of high-speed propulsion of macroparticles provides the physical basis for the "shock" initiation of controlled thermonuclear reactions in the form of microexplosions[119,120] ("impact fusion"), for which one must cause a projectile of mass ~ 0.1 g to move with a velocity ~ 150 km/s.

Among the large number of studies on laser ablative acceleration of macroparticles, we note only the results of the most recent studies, which have attained the highest velocities of propulsion. In Refs. 106 and 105, a relatively long pulse ($\tau = 3$ ns) of a neodymium laser of moderate intensity (10^{12}–10^{14} W/cm^2) was used to accelerate thin (1–50 μm) aluminum, carbon, and plastic foils to velocities $\sim 10^7$ cm/s. They showed that the optimal intensities for propulsion are those of the order of 10^{12}–10^{13} W/cm^2, which bring about a hydrodynamic efficiency of about 20% at a plasma pressure of 1–3 Mbar and a depth of burnout of the target of 0.5–3 μm. The absorption coefficient under these conditions reaches 80%, the velocity of dispersal of the corona is $3.5 \cdot 10^7$ cm/s, while its electron temperature is ~ 15 keV. Under similar acceleration conditions, Ref. 112 has analyzed the applicability of a "rocket" model and the conditions for appearance of Rayleigh-Taylor instability.

The acceleration of aluminum targets from 6 to 20-μm thick upon irradiation with light from a neodymium laser ($E \sim 100$–300 J, $\tau = 3$ ns, $I \sim 10^{13}$–$2 \cdot 10^{14}$ W/cm^2) has been studied in detail in Ref. 91. Velocities of propulsion of 50–80 km/s were attained with a hydrodynamic efficiency of 5%. A considerable heating of the target by the x-radiation of the corona, a small fraction (no more than 10^{-4}) of nonthermal electrons, and the absence of anomalies in the heat conductivity were noted.

Acceleration of foils at higher intensities of laser radiation has been studied in Ref. 147. An iodine laser ($\lambda = 1.3$ μm) of energy 150 J and pulse duration 300 ps was employed. The intensity of the radiation on the target was varied from 10^{12} to $6 \cdot 10^{15}$ W/cm^2. Films of plastics of composition $C_6H_7O_{11}$ ($\rho = 1.6$ g/cm^3) and $C_{16}O_3H_{14}$ ($\rho = 1.2$ g/cm^3) 0.1–2.0 μm thick were used as targets. Velocities up to 10^8 cm/s were obtained for foils with the initial value

$\rho d = 2\times 10^{-4}$ g/cm^2. The authors of the study note that, as the intensity is increased from $2\cdot 10^{14}$ to $5\cdot 10^{15}$ W/cm^2, the energy emitted in hard x-rays (5–50 keV) increases by three orders of magnitude. Starting with an intensity of $\sim 10^{13}$ W/cm^2, one observes an appreciable restriction of the electron heat flux, while at $I\sim 10^{15}$ W/cm^2 values $f = 0.01$ are reached.

In all the cited experiments, the question remains unelucidated of the state of the foil being propelled. Owing to the strong electron and radiation heating as well as the heating by the shock wave, most likely it exists in a plasma phase. In any case, the criteria for nondestructive acceleration[119,120] prove to be considerably exceeded.

6. CONCLUSION

The goal-directed application of high-power lasers to obtain and study matter in extreme states is a relatively new field in the physics of high energy densities. It is naturally associated with laser thermonuclear fusion, since the thermonuclear fuel must also be brought into an extreme state to initiate the fusion reactions in a microexplosion regime. Precisely the recent studies on laser thermonuclear fusion have constituted the necessary basis for application of lasers in high-pressure physics. On the other hand, laser methods are a natural continuation and development of the more traditional dynamic methods based on using explosives, light-gas "guns", and other accelerators of macroparticles. The first experiments on laser generation of high-power shock waves have convincingly demonstrated the promise in this new field. We should expect that the rapid development now evident in studies in this field will prove to be an important stimulus to high-pressure physics as a whole.

In closing the authors express their sincere gratitude to Ya. B. Zel'dovich for interesting discussions and valuable critical remarks.

[1]L. V. Al'tshuler, Usp. Fiz. Nauk **85**, 197 (1965) [Sov. Phys. Usp. **8**, 52 (1965)].
[2]S. B. Kormer, *ibid.* 94, 641 (1968) [Sov. Phys. Usp. **11**, 229 (1968)].
[3]V. E. Fortov, *ibid.* **138**, 361 (1982) [Sov. Phys. Usp. **25**, 781 (1982)].
[4]A. V. Bushman and V. E. Fortov, *ibid.* **140**, 177 (1983) [Sov. Phys. Usp. **26**, 465 (1983)].
[5]Ya. B. Zel'dovich and Yu. P. Raĭzer, Fizika udarnykh voln i vysokotemperaturnykh gidrodinamicheskikh yavleniĭ, Nauka, M., 1968 [Engl. Transl. of 1966 ed. Physics of Shock Waves and High-Temperature Hydrodynamic Phenomena, Academic Press, New York, (1966, 1967)].
[6]N. P. Kovalenko and I. Z. Fisher, Usp. Fiz. Nauk **108**, 209 (1972) [Sov. Phys. Usp. **15**, 592 (1973)].
[7]D. A. Kirzhnits, Yu. E. Lozovik, and G. V. Shpatakovskaya, *ibid.* **117**, 3 (1975) [Sov. Phys. Usp. **18**, 649 (1975)].
[8]L. V. Al'tshuler, N. N. Kalitkin, L. V. Kuz'mina, and B. S. Chekin, Zh. Eksp. Teor. Fiz. **72**, 317 (1977) [Sov. Phys. JETP **45**, 167 (1977)].
[9]A. K. McMahon and M. Ross, in: High-Pressure Science and Technology, eds. R. D. Timmerhaus and M. S. Barber, Plenum Press, New York, 1979, p. 920.
[10]E. N. Avrorin, B. K. Vodolaga, L. P. Volkov, A. S. Vladimirov, V. A. Simonenko, and B. T. Chernovolyuk, Pis'ma Zh. Eksp. Teor. Fiz. **31**, 727 (1980) [JETP Lett. **31**, 685 (1980)].
[11]L. P. Volkov, N. P. Voloshin, *et al.*, *ibid.* **31**, 546 (1980) [JETP Lett. **31**, 513 (1980)].
[12]D. A. Kirzhnits and G. V. Shpatakovskaya, Zh. Eksp. Teor. Fiz. **62**, 2082 (1972) [Sov. Phys. JETP **35**, 1088 (1972)].
[13]A. F. Nikiforov, V. G. Novikov, *et al.*, Preprint of the IPM of the Academy of Sciences of the USSR No. 172, Moscow, 1979.
[14]R. J. Trainor, H. G. Graboske, *et al.*, Lawrence Livermore Lab. Preprint UCRL-52562, 1978.
[15]H. K. Mao and P. M. Bell, Science **191**, 851 (1976); S. Block and G. Permarini, Phys. Today, Sept. 1976, p. 44.
[16]L. F. Vereshchagin, E. N. Yakovlev, *et al.*, Pis'ma Zh. Eksp. Teor. Fiz. **16**, 382 (1972); **17**, 422 (1973); **20**, 540 (1974) [JETP Lett. **16**, 270 (1972); **17**, 301 (1973); **20**, 246 (1974)].
[17]V. N. Mineev and A. G. Ivanov, Usp. Fiz. Nauk **119**, 75 (1976) [Sov. Phys. Usp. **19**, 400 (1976)].
[18]L. V. Al'tshuler, A. V. Bushman, M. V. Zhernokletov, V. N. Zubarev, A. A. Leont'ev, and V. E. Fortov, Zh. Eksp. Teor. Fiz. **78**, 741 (1980) [Sov. Phys. JETP **51**, 373 (1980)].
[19]V. K. Gryaznov, M. V. Zhernokletov, V. N. Zubarev, I. L. Iosilevskiĭ, and V. E. Fortov, *ibid.*, p. 573 [Sov. Phys. JETP **51**, 288 (1980)].
[20]R. S. Hawke, D. E. Duerre, *et al.*, Phys. Earth and Planet Inter. **6**, 44 (1972).
[21]A. I. Pavlovskiĭ, N. P. Kolokol'chikov, *et al.*, Pis'ma Zh. Eksp. Teor. Fiz. **27**, 283 (1978) [JETP Lett. **27**, 264 (1978)].
[22]R. S. Hawke, D. E. Duerre, *et al.*, J. Appl. Phys. **43**, 2734 (1972).
[23]L. V. Al'tshuler, V. N. Moiseev, *et al.*, Zh. Eksp. Teor. Fiz. **54**, 785 (1968) [Sov. Phys. JETP **27**, 420 (1968)].
[24]R. F. Trunin, M. A. Podurets, G. V. Simakov, L. V. Popov, and B. N. Moiseev, *ibid.* **56**, 1172 (1969); **62**, 1043 (1972) [Sov. Phys. JETP **29**, 630 (1969); **35**, 550 (1972)].
[25]C. E. Ragan, M. G. Silbert, and B. C. Diven, J. Appl. Phys. **48**, 2860 (1977).
[26]P. Caldirola and G. Knoepfel, eds., The Physics of High Energy Density, Academic Press, New York, 1971 (Russ. Transl., Mir, M., 1974).
[27]R. J. Trainor, J. W. Shaner, *et al.*, Phys. Rev. Lett. **42**, 1154 (1979).
[28]L. R. Veeser and J. C. Solem, *ibid.* **40**, 1391 (1978).
[29]C. E. Ragan, Phys. Rev. A **25**, 3360 (1982).
[30]S. I. Anisimov, M. F. Ivanov, and N. A. Inogamov, Preprint of the L. D. Landau Institute of Theoretical Physics of the Academy of Sciences of the USSR, Chernogolovka, 1977.
[31]A. M. Prokhorov, S. I. Anisimov, and P. P. Pashinin, Usp. Fiz. Nauk **119**, 401 (1976) [Sov. Phys. Usp. **19**, 547 (1976)].
[32]K. Brakner and S. Dzhorna, Upravlyaemyĭ lazernyĭ sintez (Controlled Laser Fusion), Atomizdat, M., 1977.
[33]H. Motz, Physics of Laser Fusion, Academic Press, New York, 1979.
[34]G. B. Zimmerman, Lawrence Livermore Lab. Report UCRL-74811, 1973.
[35]C. G. M. Van Kessel and R. Sigel, Phys. Rev. Lett. **33**, 1020 (1974).
[36]M. Van Thiel, Compendium of Shock Wave Data, Lawrence Livermore Lab. Report UCRL-50108, 1977.
[37]F. Chen, Univ. of California Preprint UCLA PPG-160, 1973.
[38]Yu. V. Afanas'ev, N. G. Basov, *et al.*, Vzaimodeĭstvie moshchnogo lazernogo izlucheniya s plazmoĭ (Interaction of Powerful Laser Radiation with a Plasma), VINITI, M., 1978 (Itogi nauki i tekhniki (Results of Science and Technology), Vol. 17).
[39]R. M. More, in: Laser Inter. and Related Plasma Phenom., Vol. 5, eds. H. Schwartz and H. Hora, Plenum Press, New York, 1981, p. 255.
[40]Lawrence Livermore Lab. Laser Program Annual Report UCRL-50021-77, 1978.
[41]R. J. Trainor, N. C. Holmes, and R. M. More, Lawrence Livermore Lab. Report UCRL-82429, 1979.
[42]G. C. M. Van Kessel, Z. Naturforsch. A **30**, 1581 (1975).
[43]R. F. Benjamin, G. H. McCall, and A. W. Ehler, Phys. Rev. Lett. **42**, 890 (1979).
[44]A. Raven, O. Willi, and P. T. Rumsby, *ibid.* **41**, 554 (1978).
[45]R. M. More, R. J. Trainor, *et al.*, Bull. Am. Phys. Soc. **23**, 893 (1978).
[46]J. W. Shaner, in: VII Intern. AIRAPT Conference, Le Cresot, 1979.
[47]I. Shkarovskiĭ, T. Dzhonston, and M. Bachinskiĭ, Kinetika chastits plazmy Atomizdat, M., 1969, [Engl. Transl.-I. P. Shkarovsky, T. W. Johnston and M. Bachinskii. The Particle Kinetics of Plasmas, Addison-Wesley, Reading, Mass., (1966)].
[48]V. B. Mintsev, V. E. Fortov, and V. K. Gryaznov, Zh. Eksp. Teor. Fiz. **79**, 116 (1980) [Sov. Phys. JETP **52**, 59 (1980)].
[49]Lawrence Livermore Lab. Laser Program Annual Report UCRL-50021-76, 1977, Sec. 4-73.
[50]B. H. Ripin, P. G. Burkhalter, *et al.*, Phys. Rev. Lett. **34**, 1313 (1975).
[51]D. A. Tidman and L. L. Burton, *ibid.* **37**, 1397 (1976).
[52]A. C. Mitchell and W. J. Nellis, Lawrence Livermore Lab. Report UCRL-83935, 1980.
[53]L. R. Veeser, J. C. Solem, and A. I. Leiber, Appl. Phys. Lett. **35**, 761 (1979).
[54]B. N. Lomakin, V. E. Fortov, *et al.*, Zh. Eksp. Teor. Fiz. **63**, 92 (1972); **69**, 1624 (1975) [Sov. Phys. JETP **36**, 48 (1973); **42**, 828 (1975)].

[55]J. M. Auerbach, D. C. Bailey, *et al.*, Lawrence Livermore Lab. Report UCRL-79636, 1977.
[56]S. I. Anisimov, Pis'ma Zh. Eksp. Teor. Fiz. **16**, 570 (1972) [JETP Lett. **16**, 404 (1972)].
[57] L. L. Wood, R. N. Killer, and J. H. Nuckolls, Lawrence Livermore Lab. Report UCRL-79610, 1977.
[58]Rutherford Lab. Annual Report RL 79-036, 1979, p. 67.
[59]L. I. Sedov, Metody podobiya i razmernosti v mekhanike (Scaling and Dimensionality Methods in Mechanics), Nauka, M., 1966.
[60]H. Graboske and L. Wong, Lawrence Livermore Lab. Report UCRL-52323, 1977.
[61]J. Dawson, P. Kaw, and B. Green, Phys. Fluids **12**, 875 (1969).
[62]D. W. Forslund, J. M. Kindel, and K. Lee, Phys. Rev. Lett. **39**, 284 (1977).
[63]K. R. Manes *et al.*, J. Opt. Soc. Am. **67**, 717 (1977).
[64]W. L. Kruer, Lawrence Livermore Lab. Report UCRL-83149, 1979.
[65]W. G. Mead *et al.*, Phys. Rev. Lett. **37**, 489 (1976).
[66]E. V. Mishin, Dokl. Akad. Nauk SSSR **215**, 565 (1974) [Sov. Phys. Dokl. **19**, 140 (1974)].
[67]Rutherford Lab. Annual Report RL 80-026, 1980.
[68]J. P. Christiansen and N. K. Winsor, J. Comput. Phys. **35**, 291 (1980).
[69]G. S. Fraley, E. J. Linnebur, *et al.*, Phys. Fluids **17**, 474 (1974).
[70]C. E. Max, C. F. McKee, and W. C. Mead, Lawrence Livermore Lab. Preprints UCRL-83542, 1979; UCRL-84019, 1980.
[71]S. I. Anisimov, Pis'ma Zh. Teor. Fiz. **12**, 414 (1970) [JETP Lett. **12**, 287 (1970)]; Zh. Eksp. Teor. Fiz. **58**, 337 (1970) [Sov. Phys. JETP **31**, 181 (1970)].
[72]K. Estabrook and W. L. Kruer, Phys. Rev. Lett. **40**, 42 (1978).
[73]R. A. Haas, W. C. Mead, *et al.*, Phys. Fluids **20**, 322 (1977).
[74]E. Fabre *et al.*, in: VIII Conf. Intern. phys. plasmas rech. fusion nucl. controlée, IAEA, Brussels. CN-38/1–4, 1980.
[75]G. V. Sin'ko, Chislennye Metody Mekhaniki Sploshnykh Sred **12**, 121 (1981); **10**, 124 (1979).
[76]V. N. Zubarev, M. A. Podurets, *et al.*, in: Detonatsiya (Detonation), OIKhF Akad. Nauk SSSR, Chernogolovka, 1978, p. 61.
[77]V. K. Gryaznov, I. L. Iosilevskiĭ, and V. E. Fortov, Pis'ma Zh. Eksp. Teor. Fiz. **8**, 1378 (1982) [*sic*].
[78]J. S. Schilling and R. N. Shelton eds., Physics of Solids under High Pressure, North-Holland, Amsterdam, 1981.
[79]L. Davison and R. A. Graham, Phys. Rep. **55**, 256 (1979).
[80]V. E. Fortov, Teplofiz. Vys. Temp. **10**, 86 (1972).
[81]E. N. Avrorin, A. I. Zuev, *et al.*, Pis'ma Zh. Eksp. Teor. Fiz. **32**, 457 (1980) [JETP Lett. **32**, 437 (1980)]; Yu. V. Afanas'ev, N. G. Basov, *et al.*, *ibid.* **21**, 150 (1975) [JETP Lett. **21**, 68 (1975)].
[82]J.Grun, R. Decoste, and B. Ripin, Naval Res. Lab. Memorandum Report 4410, 1981.
[83]R. J. Trainor, N. C. Holmes, and R. A. Anderson, in: Shock Waves in Condensed Matter-1981, eds. W. J. Nellis, L. Seaman, and R. A. Graham, Am. Inst. Phys., New York, 1982, p. 145.
[84]M. H. Key, Nature **283**, 715 (1980).
[85]C. E. Max, C. F. McKee, and W. C. Mead, Phys. Rev. Lett. **45**, 18 (1980).
[86]C. Max, R. Fabrri, and E. Fabre, Bull. Am. Phys. Soc. **25**, 895 (1980).
[87]R. J. Harrach, Y. T. Lee, *et al.*, see Ref. 83, p. 164.
[88]A. C. Mitchell and W. J. Nellis, Rev. Sci. Instrum. **52**, 347 (1981).
[89]Y. T. Lee and R. L. More, Bull. Am. Phys. Soc. **26**, 649 (1981).
[90]N. C. Holmes, R. J. Trainor, and R. A. Anderson, see Ref. 83, p. 160.
[91]Yu. A. Bondarenko, I. N. Burdonskiĭ, *et al.*, Zh. Eksp. Teor. Fiz. **81**, 170 (1981) [Sov. Phys. JETP **54**, 85 (1981)].
[92]Los Alamos Sci. Lab. Shock Wave Data, ed. S. P. March, Univ. Calif. Press, Berkeley, 1980.
[93]C. E. Ragan, B. C. Diven, *et al.*, Bull. Am. Phys. Soc. **24**, 49 (1981).
[94]L. V. Al'tshuler and A. A. Bakanova, Zh. Prikl. Mekh. Tekh. Fiz., No. 2, 3 (1981).
[95]A. K. McMahan and M. Ross, in: High-Pressure Science and Technology, eds. R. D. Timmerhaus and M. S. Barber, Plenum Press, New York, 1979, Vol. 2, p. 920.
[96]G. B. Zimmerman and W. L. Kruer, Comm. Plasma Phys. and Contr. Fusion **2**, 51 (1975).
[97]R. H. Price, M. D. Rosen, and D. L. Banner, see Ref. 83, p. 155.
[98]N. H. Burnett, G. Josin, *et al.*, Appl. Phys. Lett. **38**, 226 (1981).
[99]D. V.Giovanelli, Bull. Am. Phys. Soc. **21**, 1047 (1976).
[100]R. J. Mason, Phys. Rev. Lett. **47**, 652 (1981).
[101]B. Yaakobi and T. S. Bristov, Phys. Rev. Lett. **38**, 350 (1977).
[102]R. C. Malone, R. L. McCrory, and R. L. Morse, Phys. Rev. Lett. **34**, 721 (1975).
[103]P. D. Goldstone, R. F. Benjamin, and R. B. Schultz, Appl. Phys. Lett. **38**, 223 (1981).
[104]N. A. Ebrahim, C. Joshi, *et al.*, Phys. Rev. Lett. **43**, 1995 (1979).
[105]B. H. Ripin, R. R. Whitlock, *et al.*, *ibid.*, p. 350.
[106]B. H. Ripin, R. Decoste, *et al.*, Phys. Fluids **23**, 1012 (1980).
[107]B. Arad, S. Eliezer, *et al.*, J. Appl. Phys. **50**, 6817 (1979).
[108]J. Grun, R. Decoste, *et al.*, Appl. Phys. Lett. **39**, 545 (1981).
[109]L. C. Solem and L. R. Veeser, Los Alamos Sci. Lab. Report LASL-LA-96 9667-MS, 1977.
[110]D. Billon *et al.*, Opt. Commun. **15**, 105 (1975).
[111]C. G. M. Van Kessel, Bull. Am. Phys. Soc. **18**, 1316 (1973).
[112]Lawrence Livermore Lab. Laser Program Annual Report UCRL-50021-75, 1976, p. 64.
[113]Lawrence Livermore Lab. Laser Program Annual Report UCRL-50021-78, 1979, p. 21.
[114]K. O. Tan, D. J. James, *et al.*, Rev. Sci. Instrum. **51**, 776 (1980).
[115]R. Fedosejevs, I. V. Tomov, N. H. Burnett, G. D. Enright, and M. C. Richardson, Phys. Rev. Lett. **39**, 933 (1977).
[116]R. Fedosejevs, M. D. Burgess, *et al.*, *ibid.* **43**, 1664 (1979).
[117]B. Bezzeredes, D. W. Forslund, and E. L. Lindman, Phys. Fluids **21**, 2179 (1978).
[118]Rutherford Lab. Laser Division Annual Report RL 79-036, 1979.
[119]B. M. Manzon, Usp. Fiz. Nauk **134**, 611 (1981) [Sov. Phys. Usp. **24**, 662 (1981)].
[120]Proceedings of Impact Fusion Workshop: Los Alamos Sci. Lab. Report LA-8000-C UC-21, 1979.
[121]R. Decoste, S. E. Bodner, *et al.*, Phys. Rev. Lett. **42**, 1673 (1979).
[122]R. H. Price *et al.*, Bull. Am. Phys. Soc. **26**, 648 (1981).
[123]A. C. Mitchell and W. J. Nellis, J. Appl. Phys. **52**, 3363 (1981).
[124]See Ref. 83; results of the Research Group, Imperial College, London, Central Laser Facility, Rutherford Laboratory.
[125]A. A. Galeev and R. Z. Sagdeev, Nucl. Fusion **13**, 603 (1973).
[126]V. P. Silin, Parametricheskoe vozdeĭstvie izlucheniya bol'shoĭ moshchnosti na plazmu (Parametric Action of High-Power Radiation on a Plasma), Nauka, M., 1973.
[127]S. I. Braginskiĭ, Zh. Eksp. Teor. Fiz. **33**, 459 (1957) [Sov. Phys. JETP **6**, 358 (1958)].
[128]C. E. Max, Lawrence Livermore Lab. Report UCRL-53107, 1981.
[129]V. L. Ginzburg, Rasprostranenie élektromagnitnykh voln v plazme, Nauka, M., 1960, 2nd ed. 1967 [Engl. Transl. of 2nd ed. Propagation of Electromagnetic Waves in Plasmas, Pergamon Press, Oxford (1970)].
[130]T. W. Johnston and J. M. Dawson, Phys. Fluids **16**, 722 (1973).
[131]V. P. Silin, Zh. Eksp. Teor. Fiz. **47**, 2254 (1964) [Sov. Phys. JETP **20**, 1510 (1965)].
[132]P. Mulser and C. van Kessel, Phys. Rev. Lett. **38**, 902 (1977).
[133]D. W. Forslund, J. M. Kindel, *et al.*, *ibid.* **36**, 35 (1976).
[134]W. L. Kruer and J. M. Dawson, Phys. Fluids **15**, 446 (1972).
[135]S. I. Anisimov and M. F. Ivanov, Dokl. Akad. Nauk SSSR, **280** (1975) [Sov. Phys. Dokl. **20**, 758 (1975)].
[136]A. N. Polyudov and Yu. S. Sigov, in: Evropeĭskaya konferentsiya po vzaimodeĭstviyu lazernogo izlucheniya s veshchestvom (European Conference on Interaction of Laser Radiation with Matter), M., 1978, p. 196.
[137]W. L. Kruer and J. M. Dawson, Phys. Fluids **14**, 1005 (1971).
[138]S. I. Anisimov, M. A. Berezovskiĭ, *et al.*, Dokl. Akad. Nauk SSSR **258**, 78 (1981) [Sov. Phys. Dokl. **26**, 510 (1981)].
[139]A. N. Polyudov and Yu. S. Sigov, in: Chislennoe modelirovanie kollektivnykh protsessov v plazme (Numerical Simulation of Collective Processes in a Plasma), IPM Akad. Nauk SSSR, 1980, p. 123.
[140]A. B. Langdon, B. F. Lasinski, and W. L. Kruer, Phys. Rev. Lett. **43**, 133 (1979).
[141]V. E. Zakharov, Zh. Eksp. Teor. Fiz. **62**, 1745 (1972) [Sov. Phys. JETP **35**, 908 (1972)].
[142]S. I. Anisimov, M. A. Beresovskii, *et al.*, Phys. Lett. A **92**, 32 (1982); Preprint Inst. Autom. Electron. No. 167, Novosibirsk, 1981.
[143]R. P. Godwin, Appl. Opt. **18**, 3555 (1979).
[144]G. McClellan, P. H. Y. Lee, and G. Caporaso, Phys. Rev. Lett. **44**, 658 (1980).
[145]F. Amiranoff, R. Fabbro, *et al.*, *ibid.* **43**, 522 (1979).
[146]K. B. Mitchell and R. P. Godwin, J. Appl. Phys. **49**, 3851 (1978).
[147]F. Amiranoff, K. Eidmann, *et al.*, Max-Planck-Inst. Quant. Opt. Report MPQ-59, 1982.
[148]A. G. M. Maaswinkel, Projektgruppe für Laserforsch. Report PLF-39, 1980.
[149]C. E. Max, W. M. Manheimer, and J. J. Thomson, Lawrence Livermore Lab. Preprint UCRL-79531, 1977.
[150]S. Bodner, Phys. Rev. Lett. **33**, 761 (1974).
[151]G. Taylor, Proc. R. Soc. London Ser. A **201**, 192 (1959); S. Chandrasek-

har, Hydrodynamic and Hydromagnetic Stability, Oxford, 1961, Chap. 10.
[152]D. B. Henderson, R. L. McCrory, and R. L. Morse, Phys. Rev. Lett. **33**, 205 (1974).
[153]C. P. Verdon, R. L. McCrory, *et al.*, Phys. Fluids **25**, 1653 (1982).
[154]N. A. Inogamov, Pis'ma Zh. Tekh. Fiz. **4**, 743 (1978) [Sov. Tech. Phys. Lett. **4**, 299 (1978)].
[155]S. Z. Belen'kiĭ and E. S. Fradkin, Tr. Fiz. Inst. Akad. Nauk SSSR **29**, 207 (1965).
[156]R. L. McCrory and R. L. Morse, Phys. Fluids **19**, 175 (1976).
[157]Y.-L. Teng, R. Fedosejevs, *et al.*, Projektgruppe für Laserforschung Preprint PLF-41, 1980.
[158]F. Amiranoff, K. Eidmann, *et al.*, Max-Planck-Inst. f. Quant. Opt. Preprint MPQ-60, 1982.
[159]R. Decoste, J. C. Kieffer, *et al.*, Phys. Rev. Lett. **47**, 35 (1981).
[160]P. A. Jaanimagi, N. A. Ebrahim, *et al.*, Appl. Phys. Lett. **38**, 734 (1981).
[161]J. H. Nuckolls, L. Wood, *et al.*, Nature **239** 133 (1972).
[162]V. A Belokon', A. V. Zabrodin, *et al.*, Preprint IPM Akad. Nauk SSSR No. 39, Moscow, 1978.
[163]S. I. Anisimov, M. A. Berezovskiĭ, V. E. Zakharov, I. V. Petrov, and A. M. Rubenchik, Zh. Eksp. Teor. Fiz. **84**, 2046 (1983) [Sov. Phys. JETP **57**, 1192 (1983)].
[164]A. Chynoweth, Phys. Today **29**, No. 5, 28 (1976) [Russ. Transl. Usp. Fiz. Nauk **126**, 614 (1978)].
[165]M. A. Yates, D. B. Van Hulsteyn, *et al.*, Phys. Rev. Lett. **49**, 1702 (1982).
[166]S. P. Obenschain, J. Grun, *et al.*, *ibid.* **48**, 1402.

Translated by M. V. King